

Mechanical structure of the nucleon and the baryon octet

Ho-Yeon Won^{a,b} Hyun-Chul Kim^{a,c} June-Young Kim^d

^a*Department of Physics, Inha University, Incheon 22212, Republic of Korea*

^b*CPHT, CNRS, École polytechnique, Institut Polytechnique de Paris, 91120 Palaiseau, France*

^c*School of Physics, Korea Institute for Advanced Study (KIAS), Seoul 02455, Republic of Korea*

^d*Theory Center, Jefferson Lab, Newport News, VA 23606, USA*

E-mail: hoyeon.won@polytechnique.edu, hchkim@inha.ac.kr, jykim@jlab.org

ABSTRACT: In this study, we investigate the flavor-decomposed gravitational form factors (GFFs) of the nucleon and the baryon octet in a mean-field approach based on the large N_c limit of QCD. Our central focus lies on illuminating the distinctive role played by the separate quarks in this context. We first scrutinize the behavior of the gravitational form factors in the large N_c limit, tracing the relations governed by spin-flavor symmetry within the framework of flavor SU(3). The results are compared with those in flavor SU(2). Additionally, we quantitatively assess the fraction of light-front momentum carried by individual quark flavors within the nucleon. Notably, we unravel variations arising from the mass distribution, as evidenced through the non-conserved form factor of the nucleon, known as the cosmological constant-term $\bar{c}(q^2)$. Venturing further, we explore not only the decomposition of the total angular momentum into the orbital angular momentum and intrinsic spin, but also its flavor decomposition. Furthermore, we delve into the intricate interplay between the D -term and \bar{c} form factors, discerning their collaborative impact on the stabilization of the nucleon system. Alongside this, we undertake an analysis, questioning the assumption of “large N_c blindness” concerning $D^{u-d} \sim 0$. Our examination concludes that such an assumption finds justification predominantly within the framework of flavor SU(3) symmetry. Using the spin-flavor symmetry, the baryon octet GFFs can be easily obtained, and various sum rules between the baryon octet GFFs are discussed. Finally, we introduce the generalized electromagnetic form factors, where the flavor structure of the electromagnetic current is induced into the GFFs. Similar to the electromagnetic form factors, we find that these newly introduced form factors possess the U -spin symmetry.

Contents

1	Introduction	1
2	QCD energy-momentum tensor	5
2.1	Matrix element of the energy-momentum tensor current	6
2.2	3D distribution versus 2D light-front distribution	6
2.3	Mass distribution	7
2.4	Angular momentum distribution	8
2.5	Mechanical properties	9
3	Chiral quark-soliton model	10
3.1	Classical nucleon	10
3.2	Collective quantization	12
3.3	Matrix element of the EMT current in the large N_c limit of QCD	13
3.4	Large N_c behavior: SU(2) versus SU(3)	15
4	Numerical results	16
4.1	QCD mass distribution: mass decomposition vs LF momentum	17
4.2	QCD angular momentum distribution	19
4.3	QCD Mechanical properties	22
4.4	Flavor-decomposed GFFs of the proton	29
4.5	SU(3) spin-flavor structure and the hyperon GFFs	29
5	Conclusions and summary	36
6	Acknowledgement	38
A	EMT distributions and regularization functions	38
B	Matrix elements of the spin-flavor operators	40

1 Introduction

Strangeness in the nucleon has been one of the most crucial issues in comprehending the underlying structure of the nucleon. The European Muon Collaboration (EMC) announced the puzzling measurement that the quark intrinsic spin provides only a small portion of the proton's spin [1, 2], there has been a great amount of experimental and theoretical works (see a review [3] and references therein). It is now known that the quark intrinsic spin carries approximately 35 % of the proton's spin [3]. The rest will come from the orbital angular momenta of the quarks and gluons inside a proton. The EMC results triggered

an idea to measure the strange contributions to the electromagnetic form factors (EMFFs) of the proton [4], and the strange vector form factors were extracted from parity-violating electron-proton scattering [5–10] and theoretically (refer to a recent review and references therein for further details [11]). Although the strange magnetic moment is relatively small, it remains significant. For instance, the strange magnetic form factor at $Q^2 \simeq 0.1, \text{ GeV}^2$ was determined to be 0.30 ± 0.17 [11]. Additionally, the πN sigma term, which contributes to the nucleon mass, incorporates contributions from the strange quark. Specifically, approximately 20 % of the πN sigma term is attributed to the strange quark [12]. Furthermore, investigations have been carried out to explore the strange-quark contribution to the nucleon tensor charge [13, 14].

The role of strange quarks can also extend to the gravitational form factors (GFFs) [15, 16] of the nucleon, which provide crucial insights into the properties of the nucleon, including its mass, spin, mechanical pressure, and shear force [17, 18]. Although the concept of the GFFs was introduced about sixty years ago [15, 16], experimental access to them had been limited, so that they were regarded as a purely academic interest. However, the emergence of generalized parton distributions (GPDs) [19–22] has paved the way for extracting experimental information on the GFFs. It is possible to measure the observables related to the GFFs because the EMFFs and GFFs can be understood as the first and second Mellin moments of vector GPDs, respectively [17].

The GFFs can also be given as parametrizations for the nucleon matrix element of the energy-momentum tensor (EMT) current. In the rest frame of the nucleon, the matrix element of the temporal component of the EMT current T^{00} at zero momentum transfer $t = 0$, denoted as $A^{q,g}(0) + \bar{c}^{q,g}(0)$, is intricately linked to the decomposition of the nucleon mass into the contributions of quarks (q) and gluons (g). This decomposition, which examines the specific roles of quarks and gluons in the total mass of the nucleon, has been extensively studied [23–32]. Meanwhile, in the infinite momentum frame (IMF), the $A(t)$ form factor is understood as a light-front momentum form factor normalized to unity. The $\bar{c}^{q,g}(t)$ form factor is associated with the twist-4 GPDs [33, 34], while the $A^{q,g}(t)$ form factor is directly linked to the leading-twist vector GPDs as the second Mellin moment or to the parton distribution functions (PDFs) as the second moment. Consequently, $A(0)$ can be interpreted as the momentum fraction carried by the partons, which is the integral of the structure function over x , i.e. $A(0) = \int dx x \sum_{a=q,g} f_1^a(x)$.

The contribution of valence quarks to the nucleon PDFs is relatively well understood. However, the contribution of sea quarks is a more complex and substantial issue. For example, the Gottfried sum rule, which assumes flavor-symmetric sea quark contributions ($\bar{u} = \bar{d}$), was widely accepted. The values of the unpolarized structure functions of the neutron and proton were observed by the New Muon Collaboration (NMC) [35, 36] from deep-inelastic muon scattering on the hydrogen and deuterium targets, and confirmed by the HERMES [37] and NuSea [38] collaborations. The series of experiments revealed the violation of the Gottfried sum rule. Moreover, the study of the s -quark contribution to the $A(t)$ form factor holds the potential for gaining profound insights into sea quarks, mass decomposition, and is an ongoing area of investigation.

The $0k$ component of the EMT current is related to the angular momentum (AM),

specifically its decomposition into the orbital angular momentum (OAM) and the spin contributions of the partons. The EMT current in quantum chromodynamics (QCD) is obtained by Noether's theorem, which derives from space-time translational symmetry and is called the canonical EMT current. While this current is conserved, it lacks gauge invariance and symmetrization in the Lorentz indices. To address these limitations, a modified EMT current has been proposed by Belinfante and Rosenfeld [39, 40]. This updated EMT current includes a "superpotential" term added to the canonical EMT current, making it both symmetric and gauge invariant. In fact, the need for a symmetrized EMT arises because gravity couples to a symmetric EMT in the context of general relativity [41] (see also a review [33]). In addition, a symmetrized EMT current is related to the second Mellin moments of the GPDs, known as the Ji's sum rule [20]. Consequently, the definition of the EMT current in QCD requires physical choices that can influence the interpretation and measurement of the operators.

When dealing with distributions corresponding to the $0k$ component of the EMT current, the definition of the AM distribution requires careful consideration, as discussed in various references [18, 42, 43]. However, considerable theoretical work has been devoted to addressing this issue, as exemplified by a review by Leader and Lorcé [33]. As a result, Ji's decomposition [20], modified by the Belinfante-Rosenfeld EMT current in the context of QCD, has gained widespread acceptance as a definition of AM:

$$\frac{1}{2} = \frac{1}{2} \sum_q \Delta q + \sum_q L^q + \Delta G + L^g. \quad (1.1)$$

Δq , also denoted as the singlet axial charge $g_A^{(0)}$, is the first moment of the structure function g_1^q . $\sum_q L^q$ represents the quark OAM, and ΔG and L^g stand for the contributions of the gluon spin and gluon OAM, respectively. Several experiments on the spin structure have been carried out to measure the spin asymmetry in the polarized lepton-nucleon deep inelastic scattering (DIS) [1, 2, 44–52]. The values of the isotriplet and octet axial charges, $g_A^{(3)} = 1.2754 \pm 0.0013$ [53] and $g_A^{(8)} = 0.58 \pm 0.03$ [54], are respectively determined through measurements of the neutron β -decay and the hyperon semileptonic decays with flavor SU(3) symmetry imposed. These experimental results demonstrate that only a small fraction of the nucleon spin is carried by quarks, and the Ellis-Jaffe sum rule [55], i.e. $\Delta s = \Delta \bar{s} = 0$, is no longer valid. This indicates that the s -quark plays a crucial role in understanding the spin structure of the nucleon, with $\Delta s \sim -0.10$ [3, 56].

As for the OAM, lattice QCD calculations have obtained $L^{u+d} \sim 0.03$ and $L^{u-d} \sim -0.38$, neglecting the contributions from disconnected diagrams [57]. Additional studies of the AM in the lattice QCD have been conducted in Refs. [58–61]. The OAM is connected to the twist-3 GPDs [62–64]. However, the accurate extraction of the twist-3 GPDs from experiments and lattice QCD simulations poses significant challenges, as discussed in Ref. [33]. Nevertheless, the determination of this unknown dynamical information remains crucial for the AM sum rule, including the contributions of s quarks.

In the rest frame, the three-dimensional (3D) tensor components of the EMT current, represented as T^{ij} , encompass the 3D pressure and shear-force distributions [18]. These distributions are determined by the 3D Fourier transform of the Polyakov-Weiss D -term

form factor [65]. Unlike the form factors related to mass and spin, the precise value of the D -term is unknown yet. Initial estimations were made in the large N_c limit of QCD [66–69]. More recently, the D -term was extracted from the experimental data on deeply virtual Compton scattering (DVCS) [70] for the first time, assuming the large N_c approximation in the flavor SU(2) sector, and the pressure [71] and shear-force [72] distributions were also obtained. For a comprehensive understanding of the mechanical interpretation of the stress tensor, refer to reviews by Polyakov et al. [73], Lorcé et al. [74], and Burkert et al. [75].

It has been demonstrated that a significant portion of the D -term form factor arises from contributions of sea quarks [66, 68] or pion cloud effects [67], necessitating a relativistic quantum field theoretical approach. However, the contribution of s -quarks (non-valence quarks) to the D -term is currently unknown. Furthermore, the flavor-decomposed form factors \bar{c}^a , which also play a certain role in the equilibrium equation for the separate quark, remain completely unknown. Recently, Hatta and Strikman proposed a method to measure the s -quark contribution to the D -term through exclusive ϕ -meson lepto-production [76]. By varying the strangeness D -term, the differential cross-section was found to be sensitive to the value of the s -quark contribution to the D -term. Thus, knowledge of the s -quark contribution to the D -term is very important for the determination of the differential cross-section.

To investigate the contributions of s -quarks to mass, spin, and the D -term, we employ the chiral quark-soliton model (χ QSM), which was developed based on the pion mean-field approach. Witten proposed in his seminal papers [77, 78] that in the large N_c limit of QCD a classical baryon can be regarded as N_c valence quarks bound by a mesonic mean field that arises as a classical solution of the saddle point equation in a self-consistent manner, while the quantum fluctuations are suppressed and of order $1/N_c$. Since the classical baryon has no momentum and no good quantum numbers, the zero-mode quantization is required to restore the translational and rotational symmetries. These rotational and translational zero modes naturally give rise to the standard SU($2N_f$) spin-flavor symmetry in the large N_c limit of QCD [79–81].

The χ QSM can directly be connected to QCD via the instanton vacuum [82, 83]. The low-energy effective partition function of QCD can be derived from the instanton vacuum, realizing the spontaneous breakdown of chiral symmetry, and the relevant low-energy theorems. Since this model is a relativistic quantum-field theoretic one, the contributions of the sea quarks (Dirac continuum) naturally arise, which are crucial to yield a classical nucleon. It is important to note that the gluon degrees of freedom have been integrated out through the instanton vacuum, and their effects are incorporated into the momentum-dependent dynamical quark mass M . In the χ QSM, we switch off the momentum dependence of M and introduce a regularization to tame the divergent quark loops. The χ QSM has been successful in describing the breakdown of the Gottfried sum rule [84, 85], the light-flavor asymmetry [86–88] of polarized PDFs, and the transversity distributions [89–91]. It has also provided a satisfactory explanation for the contributions of strange quarks to axial charges [92, 93] and vector charges [94, 95]. For a comprehensive overview, refer to the reviews [96, 97].

Finally, we want to address the issue of the 3D mechanical interpretation of the GFFs.

The 3D EMT distributions have been proposed as the Fourier transform of the GFFs [18, 68]. However, the 3D interpretation of the EMT distributions has faced significant criticism [98–102]. Due to the inability to precisely localize the nucleon wave packet below the Compton wavelength, there are ambiguous relativistic corrections to the 3D distributions (see Ref.[41]). To deal with this ambiguity, a two-dimensional (2D) light-front (LF) distribution has been used [99–101]. In the current work, however, we adhere to the 3D interpretation of the EMT distributions.

As discussed in a number of works considering the large N_c limit [103, 104], the center of motion of the nucleon exhibits a non-relativistic behavior (while the nucleon itself possesses fully relativistic internal dynamics). Therefore, information about the 3D distributions is conveyed into the 2D space on the light cone with no change. The frame dependence of these distributions has been explored in Ref. [103] in the context of the large N_c limit. In addition, it was very recently found that the 3D components of the EMT can be matched with the 2D light-front components [104]. While considering the admixture of the 3D components in this matching, the Wigner rotation (Melosh rotation) effects under the Lorentz boost are suppressed in the large N_c limit. Consequently, the light-front helicity state becomes equivalent to the canonical spin state at rest.

The structure of our paper is as follows: In section 2, we recapitulate a definition of the Belinfante-Rosenfeld EMT current in QCD and express the matrix element of the EMT current, which is parametrized in terms of the GFFs. We also discuss the 3D mechanical interpretations associated with these GFFs. In section 3, we offer a brief explanation of the χ QSM and illustrate the spin-flavor properties of the QCD GFFs in flavor SU(3) symmetry. In addition, we analyze the scaling behavior of the GFFs with respect to N_c in flavor SU(3) symmetry. In section 4, we discuss the numerical results on the 3D EMT distributions and investigate the role of the strange quark in equilibrium conditions. Furthermore, we present the flavor-decomposed GFFs for the baryon octet using the spin-flavor symmetry. Finally, in section 5 we provide a summary of our work and draw conclusions based on our findings.

2 QCD energy-momentum tensor

According to Ji’s decomposition [20], the quark (q) part of the Belinfante-Rosenfeld-type QCD EMT current is expressed as

$$\hat{T}_{\text{kin},q}^{\mu\nu} = \frac{i}{2} \bar{\psi}_q \left(\gamma^\mu \overleftrightarrow{\mathcal{D}}^\nu \right) \psi_q, \quad (2.1)$$

where $\overleftrightarrow{\mathcal{D}}^\mu = \overleftrightarrow{\partial}^\mu - 2igA^\mu$ is the covariant derivative with $\overleftrightarrow{\partial}^\mu = \overrightarrow{\partial}^\mu - \overleftarrow{\partial}^\mu$. The symmetric and antisymmetric parts of the EMT current are given by the divergence of the spin density and the Belinfante-Rosenfeld EMT current, respectively [33, 42]:

$$\hat{T}_{\text{kin},q}^{[\mu\nu]} = -\partial_\alpha \hat{S}_q^{\alpha\mu\nu}, \quad \hat{T}_{\text{kin},q}^{\{\mu\nu\}} = 2\hat{T}^{\mu\nu}, \quad (2.2)$$

where $T^{\mu\nu}$ is the Belinfante-Rosenfeld EMT current. This EMT current consists of the quark (q) and gluon (g) parts and is also a conserved quantity:

$$\hat{T}^{\mu\nu} = \sum_q \hat{T}_q^{\mu\nu} + \hat{T}_g^{\mu\nu}, \quad \partial_\mu \hat{T}^{\mu\nu} = 0, \quad (2.3)$$

which means that the flavor decomposed EMT currents are not conserved. This study focuses primarily on the SU(3) flavor structure of the EMT current, so its gluon part ($\hat{T}_g^{\mu\nu}$) will not be discussed in the current work.

2.1 Matrix element of the energy-momentum tensor current

The matrix element of the EMT current can be described by four independent Lorentz-invariant functions, namely A^q , J^q , D^q , and \bar{c}^q , which are obtained by considering all possible Lorentz structures and sorting them out by using the discrete symmetries (hermiticity, time reversal, and parity). This parameterization has been studied extensively in previous works [15, 16, 105, 106] (For further information on the generalization of this parametrization, interested readers may refer to Refs. [107, 108]). The baryon matrix element of the EMT current is expressed as

$$\begin{aligned} \langle B(p', J'_3) | \hat{T}_{\mu\nu}^q(0) | B(p, J_3) \rangle = \bar{u}(p', J'_3) \left[A_B^q(t) \frac{P_\mu P_\nu}{M_B} + J_B^q(t) \frac{iP_{\{\mu\sigma\nu\}\rho} \Delta^\rho}{2M_B} \right. \\ \left. + D_B^q(t) \frac{\Delta_\mu \Delta_\nu - g_{\mu\nu} \Delta^2}{4M_B} + \bar{c}_B^q(t) M_B g_{\mu\nu} \right] u(p, J_3), \end{aligned} \quad (2.4)$$

where A^q , J^q , D^q , and \bar{c}^q are called the mass, spin, D -term, and cosmological constant term form factors of a baryon B , respectively. In this study, we utilize the shorthand notation $\{a, b\} = ab + ba$. The normalization of the one-particle state for the baryon is expressed as $\langle B'(p', J'_3) | B(p, J_3) \rangle = 2p^0 (2\pi)^3 \delta_{J'_3 J_3} \delta^{(3)}(\mathbf{p}' - \mathbf{p})$, where J_3 and J'_3 denote the spin polarizations of the initial and final states, respectively. The M_B represents the mass of a baryon, while p and p' refer to the initial and final momenta, respectively. We define $P = (p' + p)/2$ and $\Delta = p' - p$, where $\Delta^2 = t$, to represent the average momentum and the momentum transfer between the initial and final states, respectively. We express the GFFs generically as F_B^χ , where the flavor indices run over $\chi = 0, 3, 8$. They can be decomposed in terms of the quark components

$$F_B^{\chi=0} = F_B^u + F_B^d + F_B^s, \quad F_B^{\chi=3} = F_B^u - F_B^d, \quad F_B^{\chi=8} = \frac{1}{\sqrt{3}} (F_B^u + F_B^d - 2F_B^s). \quad (2.5)$$

Thus, the GFFs of a baryon are given by the sum of all quark and gluon contributions

$$\sum_{a=q,g} F_B^a(t) = F_B(t), \quad \bar{c}_B(t) = 0. \quad (2.6)$$

Note that the current conservation imposes the constraint that $\bar{c}(t)$ is zero.

2.2 3D distribution versus 2D light-front distribution

To gain insight into the mechanical interpretation of the GFFs in coordinate space, one can perform the Fourier transformation of these form factors. This approach was first explored in Ref. [18] and was inspired by the concept used in EMFFs and their charge and magnetization distributions. However, the interpretation of EMFFs and GFFs in terms of the 3D distributions has been criticized [41, 98–102, 109] due to the inherent limitations

imposed by the Compton wavelength, which prevents the precise localization of the nucleon wave packet. Consequently, this limitation introduces ambiguous relativistic corrections to the 3D distribution.

One perspective suggests that if the nucleon is treated as a non-relativistic object (where the initial and final wave packets become equivalent and well-localized), the form factor [110] can be understood as a 3D distribution. However, if one insists on using the strict definition of the distribution, we can consider the following approach: if we consider the infinite momentum frame or the light-front formalism, then ambiguous relativistic corrections are kinematically suppressed, effectively rendering the system non-relativistic. However, we have to pay the cost of losing longitudinal information, reducing the distribution to a 2D one. Another way is to take a conceptual detour in the treatment of 3D distributions. From a Wigner phase space perspective [111–114], the 3D distribution can be regarded as quasi-probabilistic, reflecting the internal dynamics of the hadron, with all ambiguous relativistic corrections encapsulated in the Wigner distributions. Furthermore, recent developments have introduced the definition of 3D spatial distributions in the zero average momentum frame [115–117].

Since the 2D IMF provides clear and unambiguous definitions of EMT distributions, we can choose to work within that frame. However, in the context of the large N_c limit, it is both natural and sufficient to focus on the 3D distribution. While the internal dynamics of the nucleon is fully described within a relativistic framework (including all the relativistic motions of the quarks), the center of motion of the nucleon is treated in a non-relativistic manner due to the $1/N_c$ suppression. This means that translational corrections, such as $\mathbf{P}^2/2M_N \sim \mathcal{O}(N_c^{-1})$, to the nucleon energy are parametrically suppressed, and the same suppression applies to the nucleon GFFs. Consequently, the soliton nature of the nucleon is inherently static and collectively non-relativistic. A related discussion of this topic can be found in Ref. [103]. Moreover, the large N_c approximation causes the equivalence between the light-front helicity state and the canonical spin state at rest. This allows one to perform *matching* [104] between the 3D components of the EMT and the 2D LF ones.

In the Breit frame, the quark and gluon components of the GFFs are determined by taking the Fourier transforms of the matrix element of the EMT current between the initial and final states of the baryon. This definition is referred to in [18]:

$$T_{\mu\nu}^{a,B}(\mathbf{r}, J'_3, J_3) = \int \frac{d^3\Delta}{(2\pi)^3 2P^0} e^{-i\Delta\cdot\mathbf{r}} \langle B(p', J'_3) | \hat{T}_{\mu\nu}^a(0) | B(p, J_3) \rangle. \quad (2.7)$$

2.3 Mass distribution

The temporal component $T_{00}^{a,B}$ of the EMT current is related to the mass distribution of quarks and gluon inside a baryon

$$\begin{aligned} \varepsilon_B^a(r) \delta_{J'_3 J_3} &:= T_{00}^{a,B}(\mathbf{r}, J'_3, J_3) \\ &= M_B \int \frac{d^3\Delta}{(2\pi)^3} e^{-i\Delta\cdot\mathbf{r}} \left[A_B^a(t) + \bar{c}_B^a(t) - \frac{t}{4M_B^2} (A_B^a(t) - 2J_B^a(t) + D_B^a(t)) \right] \delta_{J'_3 J_3}. \end{aligned} \quad (2.8)$$

By integrating the spatial components of the EMT current ($T_{00}^{a,B}$) over space, the mass of a spin-1/2 baryon at rest can be calculated as

$$\int d^3r \sum_{a=q,g} \varepsilon_B^a(r) = M_B A_B(0) = M_B, \quad (2.9)$$

with $\varepsilon_B(r) = \sum_{a=q,g} \varepsilon_B^a(r)$ and the normalized mass form factor $A_B(0) = 1$, where the contribution of \bar{c}_B to ε_B is zero by the conservation of the EMT current. The size of the mass distribution can be expressed by the mass radius. It is given by either the integral of the mass distribution or the derivative of the mass form factor $A_B(t)$ with respect to the momentum squared,

$$\langle r_{\text{mass}}^2 \rangle_B = \frac{\int d^3r r^2 \varepsilon_B(r)}{\int d^3r \varepsilon_B(r)} = 6 \frac{d}{dt} \left[A_B(t) - \frac{t}{4m_B^2} D_B(t) \right]_{t=0}. \quad (2.10)$$

2.4 Angular momentum distribution

The mixed components of the EMT current ($T_{0i}^{a,B}$) are associated with the total angular momentum distributions (sum of spin and orbital angular momentum) by the Belinfante and Rosenfeld construction. The definition of the total angular momentum distributions inside a baryon is given by the angular momentum operator in QCD as follows:

$$\begin{aligned} J_i^{a,B}(\mathbf{r}, J'_3, J_3) &:= \varepsilon_{ijk} r_j T_{0k}^{a,B}(\mathbf{r}, J'_3, J_3) \\ &= 2 \left(\hat{S}_j \right)_{J'_3 J_3} \int \frac{d^3\Delta}{(2\pi)^3} e^{-i\Delta \cdot \mathbf{r}} \left[\left(J_B^a(t) + \frac{2}{3} t \frac{dJ_B^a(t)}{dt} \right) \delta_{ij} \right. \\ &\quad \left. + \left(\Delta_i \Delta_j - \frac{1}{3} \Delta^2 \delta_{ij} \right) \frac{dJ_B^a(t)}{dt} \right]. \end{aligned} \quad (2.11)$$

In the following discussion, we will separate it into its monopole and quadrupole parts. Note, however, that the quadrupole distribution is related to the monopole distribution [18, 42, 43]. For the purpose of this discussion, we will refer to the monopole distribution [18] as the AM distribution, which can be expressed as follows

$$\rho_{J,B}^a(r) := \int \frac{d^3\Delta}{(2\pi)^3} e^{-i\Delta \cdot \mathbf{r}} \left[\left(J_B^a(t) + \frac{2}{3} t \frac{dJ_B^a(t)}{dt} \right) \right]. \quad (2.12)$$

Integrating both $J_i^{a,B}(\mathbf{r}, J'_3, J_3)$ and $\rho_{J,B}^a(r)$ in 3D space yields the spin of the baryon as follows

$$\int d^3r \sum_{a=q,g} J_i^{a,B}(\mathbf{r}, J'_3, J_3) = 2 \left(\hat{S}_i \right)_{J'_3 J_3} J_B(0) = \left(\hat{S}_i \right)_{J'_3 J_3}, \quad (2.13)$$

with $\rho_{J,B}(r) = \sum_{a=q,g} \rho_{J,B}^a(r)$. The AM form factor $J_B(0)$ is normalized to 1/2 to ensure that the integral of the AM distribution $J_i^{a,B}(\mathbf{r}, J'_3, J_3)$ over space is equivalent to the spin operator of a baryon. Note that the quadrupole component has no effect on the spin normalization. For more information on the separation of the OAM and the intrinsic spin using the QCD equation of motion, see Refs. [33, 42].

2.5 Mechanical properties

The spatial components of the EMT, denoted $T_{ij}^{a,B}$, give information about the mechanical properties of a baryon. These properties include the distributions of the pressure, $p(r)$, and shear force, $s(r)$, inside the baryon. By decomposing $T_{ij}^{a,B}$ into irreducible tensors, the pressure and shear-force distributions are connected to the rank 0 and rank 2 tensors, respectively:

$$T_{ij}^{a,B}(\mathbf{r}, J_3^i, J_3^j) = p_B^a(r) \delta^{ij} \delta_{J_3^i J_3^j} + s_B^a(r) \left(\frac{r^i r^j}{r^2} - \frac{1}{3} \delta^{ij} \right) \delta_{J_3^i J_3^j}. \quad (2.14)$$

where the pressure and shear-force distributions are defined as

$$\begin{aligned} p_B^a(r) &= \frac{1}{6M_B} \frac{1}{r^2} \frac{d}{dr} r^2 \frac{d}{dr} \tilde{D}_B^a(r) - M_B \int \frac{d^3 \Delta}{(2\pi)^3} e^{-i\Delta \cdot \mathbf{r}} \bar{c}_B^a(t), \\ s_B^a(r) &= -\frac{1}{4M_B} r \frac{d}{dr} \frac{1}{r} \frac{d}{dr} \tilde{D}_B^a(r), \end{aligned} \quad (2.15)$$

with

$$\tilde{D}_B^a(r) = \int \frac{d^3 \Delta}{(2\pi)^3} e^{-i\Delta \cdot \mathbf{r}} D_B^a(t). \quad (2.16)$$

Similarly, the pressure and shear-force distributions can be expressed as the Fourier transform of the \bar{c} and D -term form factors

$$\begin{aligned} D_B^a(t) &= 4M_B \int d^3 r \frac{j_2(r\sqrt{-t})}{t} s_B^a(r), \\ \bar{c}_B^a(t) - \frac{t}{6M_B^2} D_B^a(t) &= -\frac{1}{M_B} \int d^3 r j_0(r\sqrt{-t}) p_B^a(r). \end{aligned} \quad (2.17)$$

It should be noted that the distributions of the gluon and quark shear forces do not depend on $\bar{c}^a(t)$, while the knowledge of $\bar{c}^a(t)$ is necessary to determine the pressure distributions.

Reference [118] investigated the internal force between the $u + d$ quark and the gluon in the context of the large N_c expansion, while Ref. [119] examined the internal force between the u and d quarks. Both studies emphasize the smallness of the $\bar{c}^{q,g}$ form factors. Furthermore, the mechanical interpretation of the \bar{c} form factor was discussed in Refs.[118, 119]. The distributions of the stress tensors p_B and s_B , which represent the sum of each parton contribution ($p_B := \sum_{a=q,g} p_B^a$, $s_B := \sum_{a=q,g} s_B^a$), are strongly constrained by the conservation of the EMT current. This constraint is expressed by the equilibrium equation:

$$\frac{\partial}{\partial r} \left(\frac{2}{3} s_B(r) + p_B(r) \right) + \frac{2s_B(r)}{r} = 0, \quad (2.18)$$

which connects the pressure distribution to the shear-force one. Upon analyzing the individual contributions of the partons to these distributions, we discover an intriguing equilibrium equation that relates the quark and gluon subsystems, which is expressed by the continuity equation:

$$\sum_{a=q,g} \partial^i T_{ij}^{a,B} = \sum_{a=q,g} \frac{r_j}{r} \left[\frac{2}{3} \frac{\partial s_B^a(r)}{\partial r} + \frac{2s_B^a(r)}{r} + \frac{\partial p_B^a(r)}{\partial r} \right] = \sum_{q=u,d,s} f_{B,j}^q + f_{B,j}^g = 0, \quad (2.19)$$

where the internal force between the quarks and gluon inside the baryon is represented as

$$f_{B,j}^a = -M_B \frac{\partial}{\partial r^j} \int \frac{d^3\Delta}{(2\pi)^3} e^{-i\Delta \cdot r} \bar{c}_B^a(t). \quad (2.20)$$

As a consequence of Eq. (2.19) for a mechanically stable baryon, the sum of the internal forces $f_{B,j}^a$ between the partons must cancel out each other. Additionally, integrating Eq. (2.15) over space leads to a critical stability criterion known as the von Laue stability condition:

$$\int_0^\infty dr r^2 p_B(r) = 0. \quad (2.21)$$

This condition implies that the pressure distribution must have at least one nodal point where it becomes null. Furthermore, another stability criterion, proposed in several works [74, 120, 121], is worth mentioning. Perevalova et al. [120] introduced a local stability criterion that states a specific combination of the pressure and shear-force distributions must be positive (outward) at any given distance r :

$$\frac{2}{3}s_B(r) + p_B(r) > 0. \quad (2.22)$$

This function can be interpreted as the normal force field, while the tangential force can be expressed as $-\frac{1}{3}s_B(r) + p_B(r)$. Furthermore, the positivity of the shear-force distribution over r in Eq. (2.18), i.e., $s_B(r) > 0$, implies that $\frac{2}{3}s_B(r) + p_B(r) > 0$ is a monotonically decreasing function. To quantify the mechanical size of a baryon system, the mechanical radius is defined as:

$$\langle r_{\text{mech}}^2 \rangle_B = \frac{\int d^3r r^2 \left(\frac{2}{3}s_B(r) + p_B(r)\right)}{\int d^3r \left(\frac{2}{3}s_B(r) + p_B(r)\right)} = \frac{6D_B(0)}{\int_{-\infty}^0 D_B(t)dt}. \quad (2.23)$$

3 Chiral quark-soliton model

In this section, we briefly review the χ QSM.

3.1 Classical nucleon

The χ QSM is based primarily on two fundamental principles: chiral symmetry breaking and the large N_c limit of QCD. This model is constructed, based on the effective partition function of QCD, which is applicable in the low-energy regime. In Euclidean space, the partition function is expressed as

$$Z_{\text{eff}} = \int \mathcal{D}\psi^\dagger \mathcal{D}\psi \mathcal{D}U \exp(-S_{\text{eff}}), \quad S_{\text{eff}} = \int d^4x \psi^\dagger (i\cancel{\partial} + iMU\gamma^5 + i\hat{m}) \psi, \quad (3.1)$$

where M denotes the dynamical quark mass. It is originally given as a momentum-dependent one $M(k)$, where k stands for the quark momentum or quark virtuality. For simplicity, we switch off the momentum dependence of $M(k)$, and consider it as a free parameter. We fix its value by reproducing various nucleon form factors and the mass differences between

the nucleon and the Δ baryon. The most favorable value of M is found to be 420 MeV. \hat{m} represents the diagonal matrix of the current quark masses in the SU(3) flavor space. We assume isospin symmetry, setting $\bar{m} = m_u = m_d$. While the strange current quark mass is typically treated perturbatively, its contributions to the GFFs are found to be small. Thus, we impose the flavor SU(3) symmetry, i.e. $\bar{m} = m_s$.

Since we use the constant M , we have to tame the divergences arising from the quark-loop integrals. To deal with them, we introduce the proper-time regularization. We fix the cutoff mass Λ by fitting the pion decay constant $f_\pi = 93$ MeV, and determine the current quark mass m by reproducing the pion mass $m_\pi = 139$ MeV (see Ref. [122] for more details).

The chiral field U^{γ_5} is represented by the U field:

$$U^{\gamma_5} = \frac{1 + \gamma_5}{2}U + \frac{1 - \gamma_5}{2}U^\dagger, \quad (3.2)$$

with $U = \exp(i\pi^a\lambda^a)$. The π^a denote the pseudo-Nambu-Goldstone (pNG) fields, and λ^a designate the Gell-Mann matrices. In the pion mean-field approach, we consider the hedgehog symmetry, which is a minimal symmetry that align the spatial vector with the isospin vector in the mean field:

$$U_{\text{SU}(2)}^{\gamma_5} = \exp[i\gamma_5\hat{\mathbf{n}} \cdot \boldsymbol{\tau}P(r)], \quad (3.3)$$

where $\pi^a(\mathbf{r}) = \hat{n}^aP(r)$ with $\hat{n}^a = r^a/|\mathbf{r}|$ for $a = 1, 2, 3$, and $\pi^a(\mathbf{r}) = 0$ for $a = 4, \dots, 8$. This symmetry ensures the invariance of the pion mean field under $\text{SU}(2)_{\text{flavor}} \otimes \text{SU}(2)_{\text{spin}}$ rotations. The SU(3) chiral field in Eq. (3.1) is constructed by using the trivial embedding [78]:

$$U^{\gamma_5} = \begin{pmatrix} U_{\text{SU}(2)}^{\gamma_5} & 0 \\ 0 & 1 \end{pmatrix}, \quad (3.4)$$

where it contains the chiral field SU(2) as a subgroup: $\text{SU}(2)_{\text{flavor}} \otimes \text{SU}(2)_{\text{spin}} \otimes \text{U}(1)_Y \otimes \text{U}(1)_{Y_R}$. Here, Y and Y_R denote the hypercharge and right hypercharge, respectively.

The SU(2) one-particle Dirac Hamiltonian in this chiral theory is defined as:

$$h(U) = \gamma_4\gamma_k\partial_k + \gamma_4MU_{\text{SU}(2)}^{\gamma_5} + \gamma_4m, \quad (3.5)$$

where the strange part is obtained by replacing the chiral field by unity, i.e., $U^{\gamma_5} \rightarrow 1$. The eigenfunctions and eigenenergies are obtained by diagonalizing $h(U)$:

$$h(U)\psi_n(\mathbf{r}) = E_n\psi_n(\mathbf{r}), \quad h(1)\psi_{n^0}(\mathbf{r}) = E_{n^0}\psi_{n^0}(\mathbf{r}). \quad (3.6)$$

The Dirac spectrum E_n consists of the upper and lower Dirac continuum, which are distorted by the pion mean field from the free Dirac spectrum E_{n^0} , and the bound state level energy (or valence quark energy E_v), which emerges when the chiral field is sufficiently strong.

To compute properties such as the mass, spin and electromagnetic properties in the baryonic sector, it is necessary to evaluate the corresponding correlation function with a pion background field. This is done by performing the functional integral described in

Eq.(3.1). Having integrated the fermionic fields, we obtain the fermionic determinant. The bosonic field can only be solved approximately by using the saddle-point approximation, which holds in the large N_c approximation. In this approach, the result is determined by the integrand evaluated in the classical mesonic configuration. It is important to note that quantum fluctuations are suppressed in the $1/N_c$ expansion [77].

The classical configuration of the pion field $P_{\text{cl}}(r)$ is obtained by solving the following saddle point equation:

$$\left. \frac{\delta S_{\text{eff}}}{\delta P(r)} \right|_{P(r)=P_{\text{cl}}(r)} = 0, \quad (3.7)$$

which yields

$$M_{\text{sol}} = N_c E_{\text{val}} + E_{\text{sea}}, \quad (3.8)$$

where $N_c E_{\text{val}}$ denote the N_c valence-quark (level-quark) contribution, and E_{sea} represents the sum of the negative Dirac continuum energy with the vacuum energy subtracted. This quantity is logarithmically divergent and requires a regularization. The specific regularization functions employed are provided in Appendix A.

3.2 Collective quantization

The classical soliton does not have the well-defined momentum and spin-flavor quantum numbers. To restore the corresponding symmetries, we introduce translational and rotational zero modes. These modes allow us to replace the functional integral over the mean field U in the presence of a background pion field with the integrals over the center of mass (CM) coordinates \mathbf{X} and the rotational matrix R in flavor space:

$$\int \mathcal{D}U \mathcal{F}[U(\mathbf{x})] \rightarrow \int d^3\mathbf{X} \int \mathcal{D}R \mathcal{F} \left[TRU_{\text{cl}}(\mathbf{x})R^\dagger T^\dagger \right], \quad (3.9)$$

where the unitary transformation T represents the translational symmetry. It is important to note that both the CM coordinates $\mathbf{X}(t)$ and the rotation matrix $R(t)$ depend weakly on time. The translational zero modes endow the classical soliton with the momentum, while the rotational zero modes furnish it with the spin-flavor quantum numbers. The slow rotation and displacement of the soliton give rise to kinetic corrections that are suppressed in the $1/N_c$ expansion. When considering the baryon rest frame (e.g., the Breit frame), the translational kinetic correction does not contribute to the GFFs. Therefore, in this study we focus on the rotational zero modes to order of $\Omega \sim 1/N_c$ and the translational ones to the zeroth order. Having performed the collective quantization, we obtain the collective Hamiltonian:

$$H_{\text{coll}} = M_{\text{sol}} + \frac{1}{2I_1} \sum_{i=1}^3 \hat{j}_i^2 + \frac{1}{2I_2} \sum_{p=4}^7 \hat{j}_p^2, \quad (3.10)$$

where I_1 and I_2 represent the moments of inertia, and their explicit expressions can be found in Appendix A. The hedgehog symmetry of the mean field implies that baryon states occur

according to the selection rules: $\mathbf{J} + \mathbf{T} = 0$ and $Y_R = N_c/3$. Consequently, diagonalizing H_{coll} , we derive the rotational wave function for a baryon with spin and flavor indices:

$$\Psi_{(YTT_3)(Y_R J J_3)}^{(\mu)}(R) = \sqrt{\dim(\mu)}(-1)^{J_3 - Y_R/2} D_{(YTT_3)(Y_R J - J_3)}^{(\mu)*}(R), \quad (3.11)$$

where $D_{ab}^{(\mu)}$ denotes the SU(3) Wigner D function¹ with the corresponding SU(3) representation μ .

3.3 Matrix element of the EMT current in the large N_c limit of QCD

The matrix element of the symmetrized EMT current in Euclidean space can be calculated as follows:

$$\begin{aligned} \langle B(p', J'_3) | \hat{T}_{\mu\nu, \chi}^{\text{eff}}(0) | B(p, J_3) \rangle &= \lim_{T \rightarrow \infty} \frac{1}{Z_{\text{eff}}} \mathcal{N}^*(p') \mathcal{N}(p) e^{ip_4 \frac{T}{2} - ip'_4 \frac{T}{2}} \int d^3 \mathbf{x} d^3 \mathbf{y} e^{(-i\mathbf{p}' \cdot \mathbf{y} + i\mathbf{p} \cdot \mathbf{x})} \\ &\times \int \mathcal{D}\psi \mathcal{D}\psi^\dagger \mathcal{D}U J_B(\mathbf{y}, T/2) \hat{T}_{\mu\nu, \chi}^{\text{eff}}(0) J_B^\dagger(\mathbf{x}, -T/2) \exp[-S_{\text{eff}}], \end{aligned} \quad (3.12)$$

where J_B represents the Ioffe-type current consisting of the N_c valence quarks [123] and $\hat{T}_{\mu\nu, \chi}^{\text{eff}}(0)$ denotes the symmetrized EMT current derived from the effective chiral theory in Euclidean space. Note that $\mathcal{N}^*(p') \mathcal{N}(p')$ yields the non-relativistic normalization $2M_{\text{sol}}$, and the baryon state carries the spin, isospin, and hypercharge quantum numbers $B = \{J, J_3, T, T_3, Y\}$. The EMT current in Minkowski space can be expressed as

$$\hat{T}_{\mu\nu, \chi}^{\text{eff}}(x) = \frac{i}{4} \bar{\psi}(x) \left(\gamma_\mu \overrightarrow{\partial}_\nu + \gamma_\nu \overrightarrow{\partial}_\mu - \gamma_\mu \overleftarrow{\partial}_\nu - \gamma_\nu \overleftarrow{\partial}_\mu \right) \lambda_\chi \psi(x), \quad (3.13)$$

where λ_χ are the SU(3) Gell-Mann matrices, and the flavor singlet $\lambda_0 = \text{diag}(1, 1, 1)$ EMT current coincides with the symmetric part of the QCD EMT current.

To understand the behavior of the GFFs, we need to discuss the large N_c limit of the kinematic variables. The large N_c behavior for the nucleon mass is given as $M_B \sim \mathcal{O}(N_c) \sim M_{\text{sol}}$. The three-momentum shows $p^k \sim \mathcal{O}(N_c^0)$, and the energy scales as $p^0 \sim \mathcal{O}(N_c^1)$. Therefore, the average momentum and the momentum transfer behaves as

$$\Delta^0 \sim \mathcal{O}(N_c^{-1}), \quad \Delta^i \sim \mathcal{O}(N_c^0), \quad P^0 \sim \mathcal{O}(N_c^1), \quad P^i \sim \mathcal{O}(N_c^0). \quad (3.14)$$

In addition, the moments of inertia are given in the following order

$$I_1 \sim \mathcal{O}(N_c^1), \quad I_2 \sim \mathcal{O}(N_c^1). \quad (3.15)$$

¹We want to mention that the SU(2) Wigner D function is associated with the SU(4) spin-flavor generators, i.e., $D^{ai} \sim -4/(N_c + 2) \hat{G}^{ia} + \mathcal{O}(N_c^{-2})$ with $a, i = 1, 2, 3$. When it comes to the SU(3) Wigner D function, it can be interpreted in a similar way as the standard SU(6) spin-flavor generators \hat{G}^{ia} with $a, i = 1, \dots, 8$. See Refs. [79–81] for a detailed discussion.

In the large N_c limit, the matrix elements of the 00-, ij -, and $0k$ -components of the symmetric EMT-like current are written as

$$\begin{aligned}
\langle B(p', J'_3) | \hat{T}_\chi^{00}(0) | B(p, J_3) \rangle &= 2M_{\text{sol}}^2 \left[A_B^\chi(t) + \bar{c}_B^\chi \right. \\
&\quad \left. - \frac{t}{4M_{\text{sol}}^2} (D_B^\chi(t) - 2J_B^\chi(t)) \right] \delta_{J'_3 J_3}, \\
\langle B(p', J'_3) | \hat{T}_\chi^{ij}(0) | B(p, J_3) \rangle &= \left[\frac{\Delta^i \Delta^j - \delta^{ij} \Delta^2}{2} D_B^\chi(t) - 2M_{\text{sol}}^2 \delta^{ij} \bar{c}_B^\chi(t) \right] \delta_{J'_3 J_3}, \\
\langle B(p', J'_3) | \hat{T}_\chi^{0k}(0) | B(p, J_3) \rangle &= -2iM_{\text{sol}} \varepsilon^{klm} \Delta^l \hat{S}_{J'_3 J_3}^m J_B^\chi(t). \tag{3.16}
\end{aligned}$$

Defining the static EMT distribution in the large N_c limit

$$T_\chi^{\mu\nu}(\mathbf{r}, J'_3, J_3) = \int \frac{d^3\Delta}{(2\pi)^3 2M_{\text{sol}}} e^{-i\Delta \cdot \mathbf{r}} \langle B(p', J'_3) | T_\chi^{\mu\nu}(0) | B(p, J_3) \rangle, \tag{3.17}$$

we obtain the final expressions for the EMT form factors as the 3D Fourier transforms of the EMT distributions:

$$\begin{aligned}
\left[A_B^\chi(t) + \bar{c}_B^\chi(t) - \frac{t}{4M_{\text{sol}}^2} (D_B^\chi(t) - 2J_B^\chi(t)) \right] \delta_{J'_3 J_3} &= \frac{1}{M_{\text{sol}}} \int d^3r j_0(r\sqrt{-t}) \varepsilon_B^\chi(r), \\
\left[\bar{c}_B^\chi(t) - \frac{t}{6M_{\text{sol}}^2} D_B^\chi(t) \right] \delta_{J'_3 J_3} &= -\frac{1}{M_{\text{sol}}} \int d^3r j_0(r\sqrt{-t}) p_B^\chi(r), \\
D_B^\chi(t) \delta_{J'_3 J_3} &= 4M_{\text{sol}} \int d^3r \frac{j_2(r\sqrt{-t})}{t} s_B^\chi(r), \\
2S_{J'_3 J_3}^3 J_B^\chi(t) &= 3 \int d^3r \frac{j_1(r\sqrt{-t})}{r\sqrt{-t}} \rho_{J,B}^\chi(r), \tag{3.18}
\end{aligned}$$

where the respective distributions ε_B^χ , $\rho_{J,B}^\chi$, s_B^χ , and p_B^χ are given by

$$\begin{aligned}
\varepsilon_B^\chi(r) &= \frac{1}{\sqrt{3}} \langle D_{\chi 8} \rangle_B \mathcal{E}(r) - \frac{2}{I_1} \langle D_{\chi i} J_i \rangle_B \mathcal{J}_1(r) - \frac{2}{I_2} \langle D_{\chi a} J_a \rangle_B \mathcal{J}_2(r), \\
\rho_{J,B}^\chi(r) &= \langle D_{\chi 3} \rangle_B \left(\mathcal{Q}_0(r) + \frac{1}{I_1} \mathcal{Q}_1(r) \right) - \frac{1}{\sqrt{3}} \langle D_{\chi 8} J_3 \rangle_B \frac{1}{I_1} \mathcal{I}_1(r) - \langle d_{ab3} D_{\chi a} J_b \rangle_B \frac{1}{I_2} \mathcal{I}_2(r), \\
s_B^\chi(r) &= \frac{1}{\sqrt{3}} \langle D_{\chi 8} \rangle_B \mathcal{N}_1(r) - \frac{2}{I_1} \langle D_{\chi i} J_i \rangle_B \mathcal{J}_3(r) - \frac{2}{I_2} \langle D_{\chi a} J_a \rangle_B \mathcal{J}_4(r), \\
p_B^\chi(r) &= \frac{1}{\sqrt{3}} \langle D_{\chi 8} \rangle_B \mathcal{N}_3(r) - \frac{2}{I_1} \langle D_{\chi i} J_i \rangle_B \mathcal{J}_5(r) - \frac{2}{I_2} \langle D_{\chi a} J_a \rangle_B \mathcal{J}_6(r). \tag{3.19}
\end{aligned}$$

The $\langle \dots \rangle_B$ denotes the matrix element of the $SU(2N_f)$ spin-flavor operators between the initial and final rotational wave functions

$$\langle \dots \rangle_B = \int dR \Psi_{(Y'T'T'_3)(Y_R J' J'_3)}^{(\mu)*}(R) \dots \Psi_{(YTT_3)(Y_R J J_3)}^{(\mu)}(R). \tag{3.20}$$

The detailed expressions for the densities \mathcal{E} , \mathcal{J}_1 , \mathcal{J}_2 , etc. are given in Appendix A. In the limit $\chi \rightarrow 0$, the results for the flavor singlet EMT distributions [68, 124] are recovered as follows:

$$\varepsilon_B^0(\mathbf{r}) = \mathcal{E}(\mathbf{r}), \quad \rho_{J,B}^0(\mathbf{r}) = -\frac{1}{2I_1}\mathcal{I}_1(\mathbf{r}), \quad s_B^0(\mathbf{r}) = \mathcal{N}_1(\mathbf{r}), \quad p_B^0(\mathbf{r}) = \mathcal{N}_3(\mathbf{r}). \quad (3.21)$$

The integrals of the individual EMT distributions over 3D space satisfy the following relations:

$$\begin{aligned} \int d^3r \mathcal{E}(\mathbf{r}) &= M_{\text{sol}}, & \int d^3r \mathcal{I}_1(\mathbf{r}) &= -I_1, \\ \int d^3r \mathcal{N}_3(\mathbf{r}) &= 0, \end{aligned} \quad (3.22)$$

Using Eq. (3.22), we find that the mass and AM form factors are properly normalized to its mass and AM

$$\int d^3r \varepsilon_B^0(\mathbf{r}) = M_{\text{sol}}, \quad \int d^3r \rho_{J,B}^0(\mathbf{r}) = 1/2. \quad (3.23)$$

In addition, the last relation in Eq. (3.22) results in the von Laue condition

$$\int d^3r p_B^0(\mathbf{r}) = 0. \quad (3.24)$$

In our study, we find that the presence of the s quark has no effect on the normalizations of the EMT form factor and the von Laue condition. It is noteworthy that the mass and AM normalizations hold true regardless of the configuration of the pion field. However, the von Laue condition is only satisfied when the pion field assumes a classical configuration. This emphasizes the importance of considering the dynamical nature of the system when describing properties related to the stress tensor.

Furthermore, while the conserved EMT current ensures the normalization of the total AM, the distinction between intrinsic spin and OAM remains a significant issue to investigate carefully. We will address this aspect in our discussion of the numerical results.

3.4 Large N_c behavior: SU(2) versus SU(3)

Before we proceed to the numerical results, we discuss the behavior of the GFFs in the large N_c limit. We obtained the following relations for the SU(2) isoscalar and isovector GFFs:

$$\begin{aligned} A^{u+d}(t) &\sim O(N_c^0), & A^{u-d}(t) &\sim O(N_c^{-1}), \\ J^{u+d}(t) &\sim O(N_c^0), & J^{u-d}(t) &\sim O(N_c^1), \\ D^{u+d}(t) &\sim O(N_c^2), & D^{u-d}(t) &\sim O(N_c^1), \\ \bar{c}^{u+d}(t) &\sim O(N_c^0), & \bar{c}^{u-d}(t) &\sim O(N_c^{-1}). \end{aligned} \quad (3.25)$$

According to the $1/N_c$ expansion, the isoscalar form factors A^{u+d} , D^{u+d} , and \bar{c}^{u+d} are parametrically dominant over their isovector counterparts A^{u-d} , D^{u-d} , and \bar{c}^{u-d} by one order of N_c . Conversely, the isoscalar T^{0k} form factor (J^{u+d}) is suppressed by an order of

N_c compared to the isovector J^{u-d} form factor in the large N_c limit. These findings are in agreement with results obtained from lattice QCD simulations and models.

In the context of SU(3) symmetry, the N_c behaviors of the flavor singlet GFFs remain unchanged. However, the flavor triplet and octet GFFs show the following behaviors:

$$\begin{aligned}
A^0(t) &\sim O(N_c^0), & A^3(t) &\sim O(N_c^0), & A^8(t) &\sim O(N_c^0), \\
J^0(t) &\sim O(N_c^0), & J^3(t) &\sim O(N_c^1), & J^8(t) &\sim O(N_c^1), \\
D^0(t) &\sim O(N_c^2), & D^3(t) &\sim O(N_c^2), & D^8(t) &\sim O(N_c^2), \\
\bar{c}^0(t) &\sim O(N_c^0), & \bar{c}^3(t) &\sim O(N_c^0), & \bar{c}^8(t) &\sim O(N_c^0).
\end{aligned} \tag{3.26}$$

The N_c behaviors of the flavor triplet GFFs (A^3 , D^3 , and \bar{c}^3) increase, being equivalent to those of the flavor singlet GFFs (A^0 , D^0 , and \bar{c}^0). However, the N_c behaviors of the flavor singlet and triplet angular momenta remain unchanged. Furthermore, the N_c behaviors of the flavor octet GFFs are the same as those of the flavor triplet GFFs. The trivial embedding of the SU(2) soliton into the SU(3) space changes the N_c counting of the form factors. It brings about the difference between Eq. (3.25) and Eq. (3.26): the N_c behaviors of the isotriplet GFFs are different from those of the flavor-triplet ones.

4 Numerical results

Before delving into the numerical results for the flavor decompositions of the EMT distributions and form factors, it is crucial to acknowledge the limitations of the current approach. We have made certain assumptions regarding the rotational and translational zero modes, treating them up to corrections of $1/N_c$ and zero, respectively. Additionally, we have considered the flavor SU(3) symmetry where the strange current quark mass, m_s , is set to $m_u = m_d = m_s$. We have previously investigated the impact of m_s on the GFFs and EMT distributions, and found that while these contributions introduce some differences in the octet baryon GFFs, they are ultimately negligible, with m_s corrections approximately 10% [124]. Moreover, if we were to incorporate m_s corrections into the stress tensor T^{ij} , the von Laue condition would be violated. Consequently, we would need to artificially reconstruct the pressure distribution by solving the differential equation (2.18) related to shear-force distributions. Therefore, in the context of examining flavor structures, it is reasonable to disregard these contributions to allow for a clearer understanding of the GFFs and distributions at a glance.

It is of great importance to emphasize that we have consistently considered and incorporated $1/N_c$ corrections in the estimation of the GFFs and EMT distributions. This approach ensures that the flavor components of the GFFs and distributions are treated with equal accuracy within the $1/N_c$ expansion considered.

Lastly, we should acknowledge the potential impact of $\Omega^2 \sim 1/N_c^2$ corrections on the GFFs. These corrections lead to discernible differences in the EMT structures between the octet and decuplet baryons. However, investigating these effects falls outside the scope of the current study. Interested readers are encouraged to explore the relevant literature, specifically Refs. [120, 125, 126], for more in-depth discussions on this topic.

4.1 QCD mass distribution: mass decomposition vs LF momentum

By taking the linear combinations of the $\chi = 0, 3, 8$ components of Eq. (3.19), we can derive the flavor-singlet, -triplet, and -octet components of the mass distributions of the nucleon. It is important to note that the 3D mass distribution, defined in the instant form quantization at the rest frame, is normalized as follows:

$$A_p^\chi(0) + \bar{c}_p^\chi(0) = \frac{1}{M_{\text{sol}}} \int d^3r \varepsilon_p^\chi(r). \quad (4.1)$$

The values of each component $\chi = 0, 3, 8$ for the mass form factors (or normalization of the mass distribution) are listed as follows:

$$\begin{aligned} A_p^0(0) + \bar{c}_p^0(0) &= 1, & A_p^3(0) + \bar{c}_p^3(0) &= 0.25, & A_p^8(0) + \bar{c}_p^8(0) &= 0.47, & [\text{SU}(3)] \\ A_p^0(0) + \bar{c}_p^0(0) &= 1, & A_p^3(0) + \bar{c}_p^3(0) &= 0.24. & & & [\text{SU}(2)] \end{aligned} \quad (4.2)$$

The proton mass distribution, or the flavor-singlet mass distribution ε_p^0 , is normalized to its mass M_{sol} , which ensures that the mass form factor is normalized to $A_p^0(0) + \bar{c}_p^0(0) = 1$. Since the spin-flavor operator of the flavor-singlet component is proportional to unity, the masses of the octet baryons are all degenerate. It is worth noting that the gluon contributions are parametrically suppressed with respect to the instanton packing fraction [118, 127], allowing us to consider them negligible at the low normalization point of $\mu \sim 600$ MeV. It implies that the gluon contributions to the GFFs can be ignored throughout this study. Thus, the normalization of the nucleon mass is solely determined by the quark contributions. Furthermore, we observe that the flavor-triplet mass distribution is smaller than the flavor-singlet one. It suggests that the parametric suppression of the flavor triplet in SU(2) symmetry remains valid in flavor SU(3) symmetry, although they become parametrically equivalent in flavor SU(3). In addition, the parametric equivalence of the flavor singlet, -triplet, and -octet components in the large N_c limit is reflected by the significant value of the flavor-octet mass form factor $A_p^8(0) + \bar{c}_p^8(0)$.

By decomposing the flavor-singlet, -triplet, and -octet components, we can determine the individual quark contributions to the mass distribution of the proton. The left panel of Fig. 1 shows the 3D mass distribution of the nucleon and its flavor decomposition with the flavor SU(3) symmetry. First, they are kept positive definite at any given r

$$\varepsilon_p^{u,d,s}(r) > 0. \quad (4.3)$$

Numerically, we find that the sum of the u - and d -quark contributions, as well as the s -quark contribution, is normalized to unity when integrated over r . At the origin of the proton, the magnitudes of the mass distributions for the u -, d -, and s -quarks are found to be:

$$\varepsilon_p^u(0) = 1.11 \text{ GeV/fm}^3, \quad \varepsilon_p^d(0) = 0.69 \text{ GeV/fm}^3, \quad \varepsilon_p^s(0) = 0.10 \text{ GeV/fm}^3 \quad (4.4)$$

We observe that the u -quark contributions to the mass distribution are approximately twice as large as the d -quark contributions for the proton. This can be intuitively understood

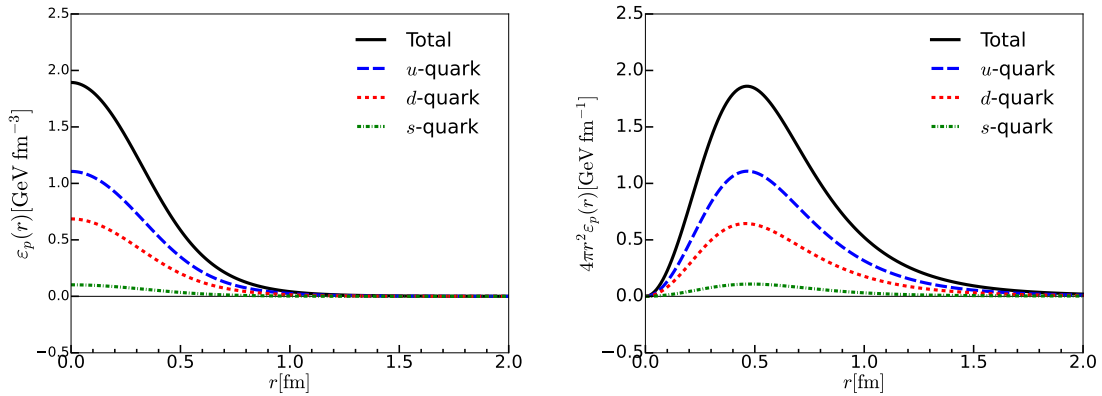


Figure 1. The 3D mass distribution of the proton and its flavor decomposition with the flavor SU(3) symmetry are plotted. The solid (black), long-dashed (blue), short-dashed (red), and dashed-dotted (green) curves denote the total, u -, d -, and s -quark contributions to the mass distributions, respectively.

by considering the number of valence quarks inside the proton. Additionally, the s -quark contribution is approximately 10% of the u -quark contribution. Notably, while the role of the u -quark inside a proton is taken by the d -quark inside a neutron, i.e., $\varepsilon_p^u(r) = \varepsilon_n^d(r)$, the s -quark contribution remains unchanged, i.e., $\varepsilon_p^s(r) = \varepsilon_n^s(r)$.

In the right panel of Figure 1, we depict the r^2 -weighted mass distributions. To quantify how far the mass distributions spread over coordinates space, we introduce the 3D mass radii. In the flavor SU(3) symmetry, the radius of the mass distribution is given by:

$$\langle r_{\text{mass}}^2 \rangle_p = 0.54, \quad (4.5)$$

which is equivalent to the radius in the flavor SU(2) symmetry. It is important to note that, as discussed in Refs. [121, 124], the mass radius is smaller than the charge radius.

Next, we consider the individual quark contributions to the proton mass, which are found to be:

$$\begin{aligned} A_p^u(0) + \bar{c}_p^u &= 0.59, & A_p^d(0) + \bar{c}_p^d &= 0.35, & A_p^s(0) + \bar{c}_p^s &= 0.06, & [\text{SU}(3)] \\ A_p^u(0) + \bar{c}_p^u &= 0.62, & A_p^d(0) + \bar{c}_p^d &= 0.38, & & & [\text{SU}(2)] \end{aligned} \quad (4.6)$$

We find that the contribution from the sea quarks (s -quark contribution) accounts for approximately 5% of the proton mass, which is relatively small.

As mentioned in the introduction, in contrast to instant form (IF) quantization at the rest frame, the form factor $A_p^q(t)$ (the 2D Fourier transform of the LF momentum form factor) is solely responsible for the LF momentum distribution. The quantity $A_p^q(0)$ represents the momentum fraction carried by the quarks within the proton. Mathematically, it is related to the unpolarized PDFs in the forward limit $t \rightarrow 0$ and $\xi \rightarrow 0$ (or the second

Mellin moments of the vector GPDs):

$$\int dx x f_1^q(x) = A_p^q(0), \quad \int dx x \sum_q f_1^q(x) = 1. \quad (4.7)$$

Subtracting the \bar{c}^q form factor obtained from the T^{ij} component of the EMT current from the IF mass form factor $A_p^q(0) + \bar{c}_p^q(0)$, we obtain LF momentum form factors $A_p^q(0)$:

$$\begin{aligned} A_p^u(0) &= 0.65, & A_p^d(0) &= 0.34, & A_p^s(0) &= 0.01, & [\text{SU}(3)] \\ A_p^u(0) &= 0.66, & A_p^d(0) &= 0.34, & & & [\text{SU}(2)] \end{aligned} \quad (4.8)$$

While the sum over all parton contributions ensures the correct normalization of the LF momentum sum rule, the integrals of the individual quark mass distributions over 3D space (Eq.(4.1)) cannot be interpreted as the longitudinal momentum fraction carried by the partons unless the information on the pressure distributions related to the \bar{c}^q form factor is provided beforehand. The definitions of the mass and pressure distributions in the context of the thermodynamics have been discussed in Refs. [23, 74].

Interestingly, our findings indicate that for any given parton ($a = q, g$), it can generally be said that if \bar{c}_p^a is positive (negative), then the fraction of proton mass M_p^a attributed to that parton is greater (smaller) than the fraction of proton momentum carried by the parton $\langle x \rangle_a$:

$$\begin{aligned} \bar{c}_p^a(0) > 0 &\quad \rightarrow \quad M_p^a/M_p > \langle x \rangle_a, \\ \bar{c}_p^a(0) < 0 &\quad \rightarrow \quad M_p^a/M_p < \langle x \rangle_a. \end{aligned} \quad (4.9)$$

If $\bar{c}_p^q(0)$ is zero, we get the trivial relation: $M_p^a/M_p = \langle x \rangle_a$. In the χ QSM, we have listed the proportions of the proton mass taken up by the u -, d -, and s -quarks compared to the proton momentum fraction carried by the u -, d -, and s -quarks:

$$\begin{aligned} M_p^u/M_p & [59.5\%] < \langle x \rangle_u [64.9\%], \\ M_p^d/M_p & [34.5\%] > \langle x \rangle_d [33.6\%], \\ M_p^s/M_p & [6.0\%] > \langle x \rangle_s [1.5\%], \end{aligned} \quad (4.10)$$

where M_p^q and $\langle x \rangle_q$ are always positive definite. We discover the inequalities between M_p^q/M_p and $\langle x \rangle_q$ which are determined by the signs of $\bar{c}_p^q(0)$. In particular, the fraction of the proton mass M_p^s/M_p attributed to the s -quark is about four times larger than the momentum fraction $\langle x \rangle_s$ carried by the s quark.

4.2 QCD angular momentum distribution

By taking the components $\chi = 0, 3, 8$ from equation (3.19), we obtain the flavor-singlet, -triplet, and -octet AMs. While the flavor-singlet AM is appropriately normalized to $J_p^0(0) = 1/2$, given by

$$J_p^0(0) = \int d^3r \rho_{J,p}^0(r) = \frac{1}{2}, \quad (4.11)$$

the flavor-triplet and -octet components are not constrained by conserved quantities and are estimated as follows:

$$\begin{aligned} J_p^0 &= 0.50, & J_p^3 &= 0.58, & J_p^8 &= 0.22, & [\text{SU}(3)]. \\ J_p^0 &= 0.50, & J_p^3 &= 0.55, & & & [\text{SU}(2)]. \end{aligned} \quad (4.12)$$

The parametrically large value of the flavor-triplet AM in the flavor SU(2) symmetry is retained in the flavor SU(3) symmetry. Furthermore, the flavor-octet component exhibits the same order of N_c as the flavor-triplet component, but numerically it is approximately a half of its magnitude.

Figure 2 illustrates the individual flavor-decomposed AM distributions inside the proton, utilizing the relations provided in Eq. (2.5). Notably, the u - and s -quark distributions exhibit positive values throughout the range of r , while the d -quark distribution is negative. It implies that the polarization of the s -quark aligns parallel to that of the u -quark, whereas the d -quark polarization aligns in the opposite direction to that of the u -quark. The right panel of Fig. 2 shows the AM distributions weighted by r^2 . When these 3D AM

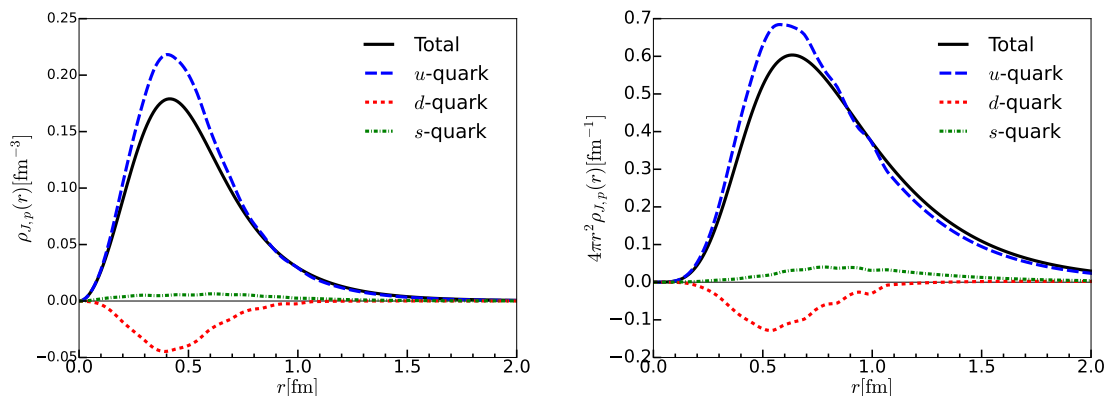


Figure 2. The 3D AM distribution of the nucleon and its flavor decomposition with the flavor SU(3) symmetry are drawn. The solid (black), long-dashed (blue), short-dashed (red), and dashed-dotted (green) curves denote the total, u -, d -, and s -quark contributions to the AM distributions, respectively.

distributions are integrated over r , the resulting values are shown below:

$$\begin{aligned} J_p^u &= 0.52, & J_p^d &= -0.06, & J_p^s &= 0.04, & [\text{SU}(3)]. \\ J_p^u &= 0.53, & J_p^d &= -0.03, & & & [\text{SU}(2)]. \end{aligned} \quad (4.13)$$

As expected, the majority of the total AM is carried by the u -quark, whereas the d -quark and s -quark give only minor contributions. These results are in line with the predictions from the SU(2) version of the χ QSM [119] and are compatible with findings from lattice QCD simulations [57]. A comprehensive analysis of the scale evolution of the AM form factors can be found in Refs. [128, 129].

In comparison with the results obtained from the SU(2) χ QSM [68, 119, 130], we observe that while the contribution of the u -quark to the total AM remains nearly unchanged, the polarization of the d -quark contribution is slightly enhanced. This suggests that the s quark is polarized in the opposite direction to the d quark, effectively canceling each other out and keeping the total AM at 1/2. Interestingly, we found that the magnitude of the s quark contribution to the total AM is nearly equal to that of the d quark contribution. However, a non-trivial question arises regarding the decomposition of AM into spin and OAM. According to the Ji's relation [17], the total AM can be expressed as the sum of the intrinsic spin and the OAM:

$$J = \frac{1}{2} \sum_q \Delta q + \sum_q L^q. \quad (4.14)$$

where we focus on the quark contributions, since the gluon contributions are parametrically suppressed in the QCD instanton vacuum [127, 131]. In the χ QSM, the antisymmetric part of the $0k$ component of the Ji's EMT current captures the spin of the s -wave quarks, while the non-symmetric part accounts for the quark AM with OAM $L = 1$. This implies that the static quark spin and the relativistic motion of the quark explain the intrinsic spin and OAM, respectively. Remarkably, we find that 50% of the flavor-singlet AM is due to the relativistic motion of the quarks inside the nucleon:

$$\frac{1}{2} = \frac{1}{2} \sum_q \Delta q + \sum_q L^q = 0.23 + 0.27. \quad (4.15)$$

It is worth noting that the effect of corrections due to the strange quark mass (m_s) on the AM decomposition has been estimated in Ref. [124] and found to be negligible, with only a few percent effect on the proton. Furthermore, in the χ QSM, the validity of Ji's relation for the flavor-singlet component has been analytically proven in Refs. [68, 132], even in the presence of flavor SU(3) symmetry breaking [124]. However, a careful treatment is required to investigate the separate contributions of quark flavors to the OAM and intrinsic spin, as discussed in Ref. [133].

The effective chiral action can be divided into a real part and an imaginary part. The real part is an ultraviolet (UV) quantity, while the imaginary part is free from UV divergence. Understanding the origin of UV divergence is crucial for determining the regularization functions. For instance, the baryon number density solely arises from the imaginary part and does not require any regularization. This can easily be demonstrated by performing the gradient expansion of the effective action with respect to the pion momentum. For further details, we refer to Refs.[96, 134]. Similarly, the total angular momentum does not require a regularization, as evidenced by the gradient expansion. However, when the total angular momentum is decomposed into the contributions of OAM L^{u-d} and intrinsic spin $S^{u-d} = g_A^{u-d}/2$, they become UV divergent quantities and must be regularized. Notably, the isovector axial-vector charge is a UV divergent quantity [96]. Hence, it is expected that the individual values of S^{u-d} and L^{u-d} would be enhanced and not reliable observables when starting from the EMT current. Thus, it is important to consider these limitations when interpreting the values of OAM and intrinsic spin. On the other hand, the divergent

parts of both S^{u-d} and L^{u-d} exactly cancel out, ensuring the validity of the prediction for J^{u-d} . It should be noted that for the flavor-singlet L^{u+d} and J^{u+d} , which are UV divergent quantities, it is relatively safe to decompose the total angular momentum into OAM and intrinsic spin.

Second, in the χ QSM, the Ji's relation for the flavor-triplet is spoiled. As discussed in Refs. [135, 136], the presence of the interacting term MU^{γ_5} introduces a modification to the Ji's relation (4.14) through an additional term δJ_p^{u-d} [135, 136]:

$$J_p^{u-d} = L_p^{u-d} + S_p^{u-d} + \delta J_p^{u-d}, \quad (4.16)$$

where δJ^{u-d} is proportional to the dynamical quark mass M . Furthermore, the second moment of the chiral-odd twist-3 quark distribution $e^{u+d}(x)$ deviates from the QCD relation due to the presence of an additional term β [137, 138]:

$$\int_{-1}^1 dx x e^{u+d}(x) = \frac{m}{M_N} N_c + \frac{M}{M_N} \beta. \quad (4.17)$$

We expect that the origin of this discrepancy may arise from the lack of the knowledge of the proper matching the QCD operator with the twist-3 effective operator [139]. Consequently, the decomposition of the flavor-decomposed AM into intrinsic spin and OAM becomes ambiguous. For further details, refer to Ref. [33]. Therefore, we will not present the corresponding results in this study.

4.3 QCD Mechanical properties

The ij component of the EMT is related to the pressure and shear-force distributions by the 3D Fourier transform and provides crucial information for understanding the stability conditions of the nucleon. To fully interpret these mechanical properties, knowledge of both the \bar{c} and D term form factors is required. A well-known stability condition, known as the von Laue condition, arises from the conservation of the EMT current. Similar to the normalization of the mass and spin of the baryon, the von Laue condition serves as a normalization condition for the stress tensor.

In general, the von Laue condition must be satisfied in the Breit frame with $J'_3 = J_3$:

$$\begin{aligned} \int d^3r \sum_{a=q,g} p_p^a(r) &= \left. \frac{\langle p(p', J_3) | \delta_{ij} \hat{T}_{ij}^a | p(p, J_3) \rangle}{6P^0} \right|_{t=0} \\ &= M_p \sum_{a=q,g} \left[-\bar{c}_p^a(t) + \frac{t}{6M_p^2} D_p^a(t) \right] \Big|_{t=0} = 0, \end{aligned} \quad (4.18)$$

where the pressure is defined by the monopole contribution to the ij component of the EMT, given by $T^{ij} \propto \delta^{ij}$. It implies that the pressure distribution (2.17) depends on both the \bar{c} and D -term form factors:

$$\langle p(p', J_3) | \hat{T}_{ij}^a | p(p, J_3) \rangle = 2P^0 M_p \delta_{ij} \left[-\bar{c}_p^a(t) + \frac{t}{6M_p^2} D_p^a(t) \right] + \dots \quad (4.19)$$

Here, the ellipsis denotes the quadrupole components in the momentum transfer Δ^i . Thus, Eq. (4.18) asserts that the sum of the quark and gluon contributions to the \bar{c} form factors must be zero in the forward limit $\Delta = 0$ in order to satisfy the von Laue condition:

$$\sum_{a=q,g} \bar{c}_p^a = 0. \quad (4.20)$$

In other words, there exists a one-to-one correspondence between the von Laue condition and the condition $\sum_{a=q,g} \bar{c}^a = 0$ (4.20). Interestingly, this condition (4.20) can be viewed as an equilibrium equation between the quark flavor and gluon subsystems, expressed as $\bar{c}^{u+d+\dots}(t) + \bar{c}^g(t) = 0$, or in position space as Eq. (2.19); refer to Refs. [118, 119] for further details.

Returning to the χ QSM, as explained earlier, the gluon contributions are suppressed at low normalization points. Consequently, the subsystem consisting of the quark flavor and gluon reduces to the quark flavor subsystem alone. This reduction is supported by the analytical proof of the global stability condition in Ref. [68], which considers only u and d quarks. Importantly, this result holds even in the case of flavor SU(3) symmetry, since the expression for the SU(2) isoscalar pressure distribution [68, 119, 124] coincides with that of the SU(3) flavor-singlet pressure distribution [124]:

$$\int d^3r p_p^{u+d+s}(r) = 0. \quad (4.21)$$

This implies that instead of Eq. (4.20) we have an equilibrium equation between the quark flavor subsystems [119], represented as $\bar{c}_p^{u+d+\dots} = 0$, or Eq. (2.19) in position space.

In the χ QSM, the flavor-singlet D -term form factor can be extracted from both the pressure and shear-force distributions through the 3D Fourier transform (2.17), benefiting from the fact that \bar{c}^{u+d+s} is zero (4.20). This indicates that the two distributions are not independent. It is worth noting that the self-consistent determination of the pion configuration is crucial for the pressure and shear-force distributions to naturally satisfy the differential equation (2.18), which leads to the extracted D -terms from the pressure and shear-force distributions being identical. For more detailed information, refer to Refs. [67, 68, 119, 124, 130, 140].

For the flavor-triplet and -octet pressure components, the absence of conserved quantities leads to the violation of their von Laue conditions. This violation occurs due to the non-zero values of the $\bar{c}_p^{3,8}(0)$ form factors:

$$\int d^3r p_p^{3,8}(r) = -M_N \bar{c}_p^{3,8}(0). \quad (4.22)$$

While the flavor-triplet and -octet shear force distributions are associated with their respective D -term form factors, the flavor-triplet and -octet pressure distributions involve a combination of both \bar{c} and D -term form factors. Consequently, the two distributions are independent of each other. Thus, unlike the flavor-singlet distributions, there is no inherent connection between the shear force and pressure distributions through the differential equation (2.18).

The values of the flavor triplet and octet \bar{c} form factors are determined as follows:

$$\begin{aligned} \bar{c}_p^0(0) &= 0, & \bar{c}_p^3(0) &= -0.060, & \bar{c}_p^8(0) &= -0.080, & [\text{SU}(3)] \\ \bar{c}_p^0(0) &= 0, & \bar{c}_p^3(0) &= -0.07. & & & [\text{SU}(2)] \end{aligned} \quad (4.23)$$

We find that $\bar{c}_p^3(0)$ is comparable to $\bar{c}_p^8(0)$ and both values are negative but relatively small. These magnitudes are approximately four times larger than the internal forces between the quark and gluon subsystems ($\bar{c}^g(0) \sim -0.014$ [118]).

Additionally, we obtain the flavor singlet, triplet, and octet D -term form factors by Fourier transform of the shear-force distributions:

$$\begin{aligned} D_p^0(0) &= -2.531, & D_p^3(0) &= 0.063, & D_p^8(0) &= -0.697, & [\text{SU}(3)] \\ D_p^0(0) &= -2.531, & D_p^3(0) &= 0.295. & & & [\text{SU}(2)] \end{aligned} \quad (4.24)$$

Burkert *et al.* [71] analyzed the experimental data on DVCS, and extracted the D -term form factor using the large N_c assumption while neglecting s -quark contributions. In the flavor SU(2) sector, we observe that the isovector component of the D -term is significant. On the other hand, in the flavor SU(3), the flavor-triplet D -term is found to be almost zero, i.e., $D_p^3 \sim 0$. This indicates that the large N_c assumption is only applicable in the flavor SU(3) sector. This finding is consistent with Ref. [141]. In lattice QCD simulations [58, 59], the value of the isovector D -term is found to be very small with a negative sign, which differs from the result in the χ QSM. However, lattice QCD calculations suffer from substantial uncertainties, leaving the sign of the isovector D -term undetermined.

We obtain the flavor-decomposed pressure and shear-force distributions by linearly combining the $\chi = 0, 3, 8$ components. The resulting distributions are depicted in Figure 3. The values of the flavor-decomposed pressures at the center of the proton are given by

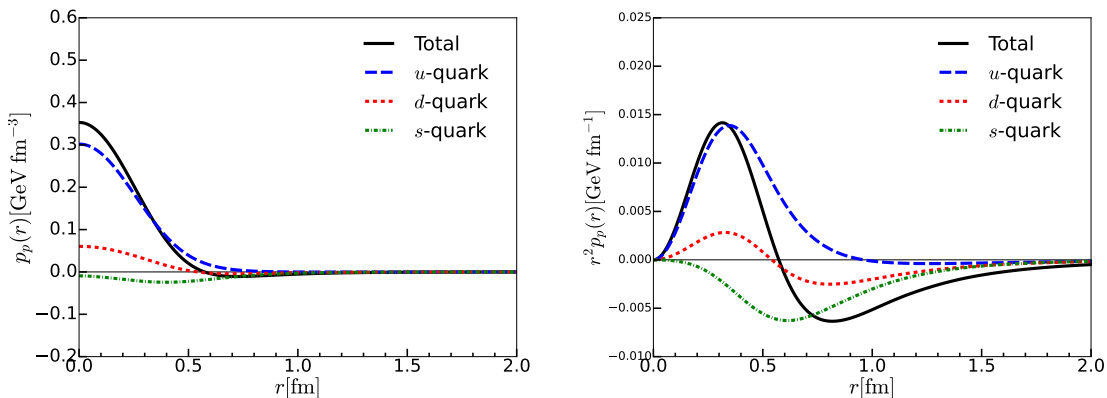


Figure 3. The 3D pressure distribution of the nucleon and its flavor decomposition with SU(3) symmetry are plotted. The solid (black), long-dashed (blue), short-dashed (red), and dashed-dotted (green) curves denote the total, u -, d -, and s -quark contributions to the pressure distributions, respectively.

$$p_p^u(0) = 0.30 \text{ GeV/fm}^3, \quad p_p^d(0) = 0.06 \text{ GeV/fm}^3, \quad p_p^s(0) = -0.01 \text{ GeV/fm}^3. \quad (4.25)$$

The dominance of the u -quark in the central region is evident, as valence quarks tend to cluster in the core. Interestingly, while the repulsive forces are governed by the u and d quarks, the attractive force is exerted by the s -quark in the core. Furthermore, it is intriguing to examine the locations of the nodal points $(r_0)_p^q$ of the flavor-decomposed pressure for the u -, d -, and s -quarks:

$$(r_0)_p^s > (r_0)_p^u > (r_0)_p^d \quad (4.26)$$

with

$$(r_0)_p^u = 0.96, \quad (r_0)_p^d = 0.54, \quad (r_0)_p^s = 5.74. \quad (4.27)$$

As depicted in Fig. 3, the inner part of the pressure is positive while the outer part is negative for the u and d quarks. This implies that the inner part of the nodal point governs the repulsive force, while the outer part governs the attractive force. Specifically, the nodal point for the u -quark is located farther away from the center, indicating the dominance of the repulsive force (valence core). The nodal point of the d -quark is closer to the center than that of the u quark, resulting in a balance between the repulsive and attractive forces, as reflected in the similarity between the nodal point of the total pressure and that of the d -quark. On the other hand, the inner part of the s -quark pressure is negative, and the nodal point is far away from the center. This fact suggests that the attractive force predominantly arises from the non-valence quark, thus contributing to the stability of the nucleon.

These observations can be quantified either by substituting the flavor-decomposed values (4.23) into Eq. (4.22), or by directly integrating the pressure distribution $p_p^q(r)$ over r :

$$\int d^3r p_p^u(r) = 0.068 \text{ GeV}, \quad \int d^3r p_p^d(r) = -0.012 \text{ GeV}, \quad \int d^3r p_p^s(r) = -0.057 \text{ GeV}. \quad (4.28)$$

where

$$\begin{aligned} \bar{c}_p^u(0) &= -0.054, & \bar{c}_p^d(0) &= 0.009, & \bar{c}_p^s(0) &= 0.045, & [\text{SU}(3)] \\ \bar{c}_p^u(0) &= -0.04, & \bar{c}_p^d(0) &= 0.04. & & & [\text{SU}(2)] \end{aligned} \quad (4.29)$$

We have indeed found that the u -quark predominantly contributes to the repulsive force, while the d - and s -quarks are mainly responsible for the attractive force. Remarkably, the attractive and repulsive forces exerted by the d -quark are well balanced. Therefore, the internal pressure can be interpreted as follows: the majority of the valence quarks (primarily the u -quark) tend to escape due to the Pauli exclusion principle, while the minority of quarks (the s - and d -quarks) confine the majority of the valence quarks from the outer region.

In Fig. 4, the flavor-decomposed shear-force distributions are drawn. All the flavor-

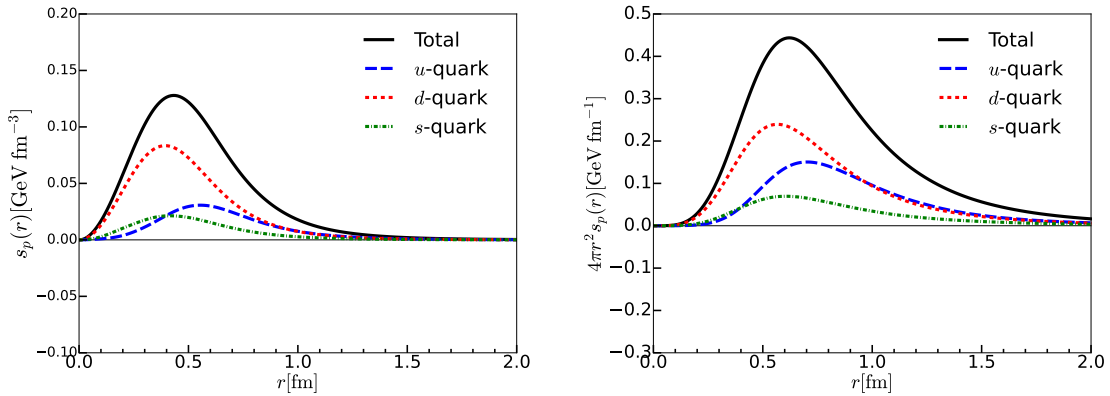


Figure 4. The shear-force distribution of the nucleon and its flavor decomposition with the flavor SU(3) symmetry are drawn. The solid (black), long-dashed (blue), short-dashed (red), and dashed-dotted (green) curves denote the total, u -, d -, and s -quark contributions to the pressure distributions, respectively.

decomposed shear-force distributions have been determined to be positive throughout the range of r . This positive definiteness of the shear force distribution, $\sum_q s_p^q(r) > 0$, leads to the inequality [68, 73, 74, 120]:

$$\frac{2}{3}s_p(r) + p_p(r) > 0, \quad (4.30)$$

which arises from the equilibrium equation (2.19) relating the pressure distribution to shear-force one. This force can be interpreted as a normal force $F_r^q(r)$ acting on an infinitesimal area, in conjunction with the tangential forces $F_\phi^q(r)$. The normal force, as well as the tangential forces, can be obtained by contracting the ij -components of the EMT distributions with the normal vector \hat{r} and the tangential vector $\hat{\phi}$, respectively [120]:

$$F_{r,p}^q(r) = 4\pi r^2 \left[\frac{2}{3}s^q(r) + p^q(r) \right], \quad F_{\phi,p}^q(r) = F_{\theta,p}^q(r) = 4\pi r^2 \left[-\frac{1}{3}s^q(r) + p^q(r) \right]. \quad (4.31)$$

As discussed in Eq. (4.22), the flavor-triplet and -octet components do not satisfy the von Laue condition, indicating a breakdown of the rigid relation between the pressure and shear-force distributions described by the equilibrium equation (2.19) (or the D -term form factor (2.15)). Consequently, the positivity of shear-force distributions for individual quark flavors does not guarantee the positivity of the corresponding normal force distributions. This is illustrated in Figs. 5 and 6, where the normal force of the s -quark becomes negative, inspite of the fact that the shear-force distribution for the s -quark are positive all over r in Fig. 4. However, the positivity of the sum of contributions from separate quark flavors to the shear-force distribution ensures the positivity of the normal force distributions, known as the local stability condition [73, 74, 120]. Regarding the tangential force, similar behaviors are

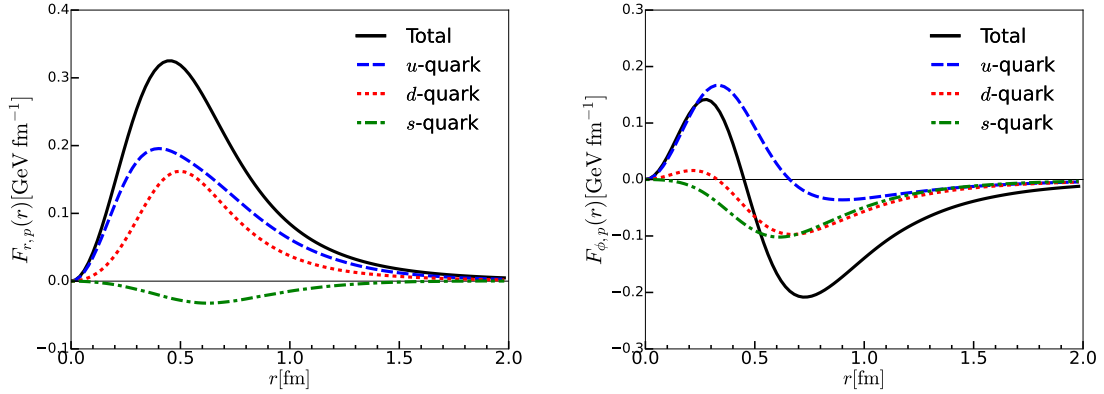


Figure 5. The normal and tangential force distributions of the nucleon and its flavor decomposition with the flavor SU(3) symmetry are drawn. The solid (black), long-dashed (blue), short-dashed (red), and dashed-dotted (green) curves denote the total, u -, d -, and s -quark contributions to the pressure distributions, respectively.

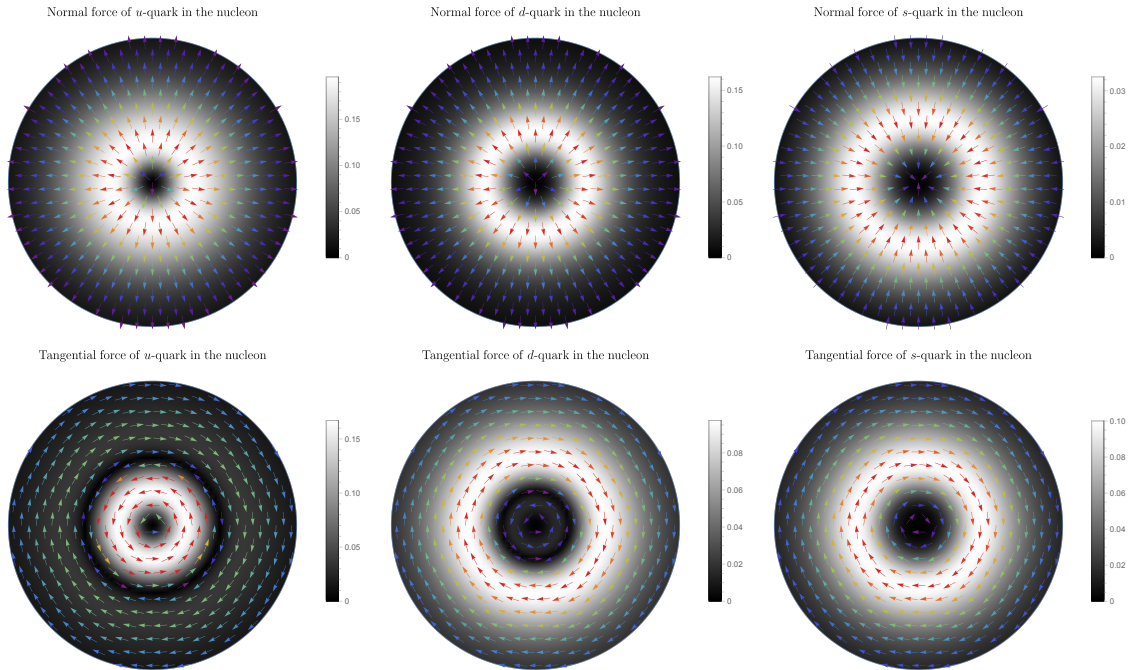


Figure 6. Visualizations of the profiles for the normal and tangential force distributions inside the nucleon for each quark flavor.

observed for the d - and s -quarks. Notably, the integral of the tangential force distributions for all quark flavors over r is found to be zero, which is referred to as the von Laue condition for the 2D subsystem. It is important to note that this differs from the 2D von Laue stability condition on the light-cone [74, 142–144].

We want to briefly discuss the close relation between the 3D BF and 2D LF stability conditions. As mentioned earlier in the introduction and Section 2, a question arises as to whether the stability condition established in the 3D BF framework holds true in the 2D LF framework. So far, we have focused on providing information regarding the 3D distributions and their associated stability conditions. Interestingly, it has been demonstrated that when considering longitudinally polarized nucleon spin, the 3D stability conditions can be directly translated into the 2D LF framework through the use of the Abel transformation [142, 143]. However, for higher-spin particles, the direct connection between the 2D LF and 3D BF distributions becomes less clear [113, 145, 146]. Therefore, in the case of the nucleon, providing the 3D BF distributions is sufficient to examine the criteria for the stability conditions.

We are now ready to delve into the mechanical interpretation of the \bar{c} form factor, which leads to deviations from the well-established stability conditions. As discussed in Section 2, Eqs. (2.19) and (2.20) elucidate the intricate interplay of internal forces between the subsystems of separate quark flavors within the nucleon. The profile of the three-dimensional (3D) distribution $f_{p,j}^q$, as described in Eq. (2.20), is visualized in Fig. 7, while

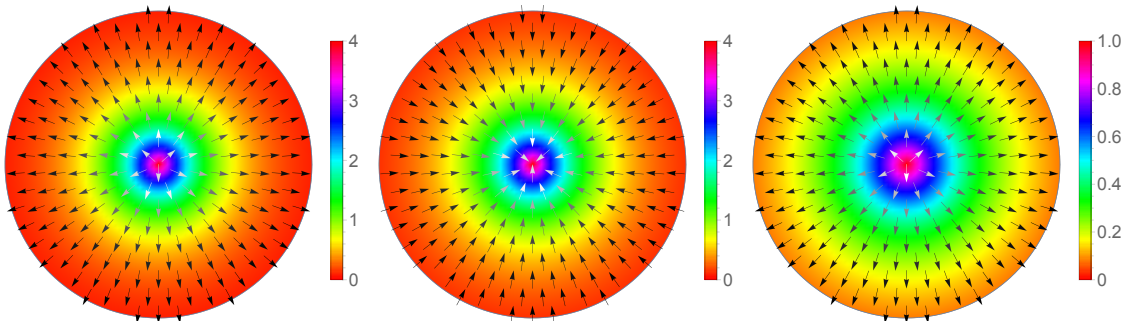


Figure 7. The internal force distributions between the quark-flavor subsystems inside the nucleon are plotted. The left, middle, and right panels show the u -, d -, and s -quark contributions to the internal force distributions, respectively.

its magnitude is depicted in Fig. 8. The force exerted by the u -quark ($\bar{c} < 0$) is directed toward the center of the nucleon, while the forces exerted by the d - and s -quarks ($\bar{c}^{d,s} > 0$) result in stretching. Consequently, we can infer that the d - and s -quarks are compressed by the u -quark subsystem. A similar interpretation was made in a study involving the quark-gluon subsystem, where the gluon forces ($\bar{c}^g < 0$) were observed to squeeze the quark subsystem ($\bar{c}^{u+d} > 0$) [118]. It is important to note that the sum of $f_p^q(r)$ must necessarily be zero over r .

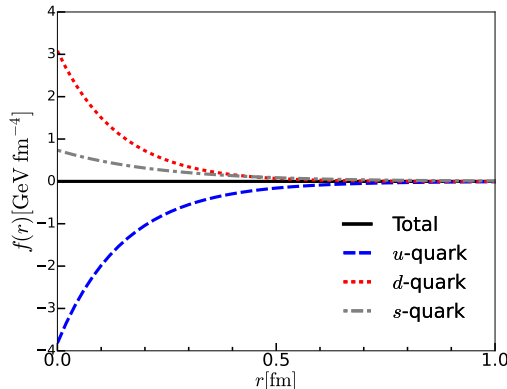


Figure 8. The internal force distributions between the quark-flavor subsystems inside the nucleon are drawn. The solid (black), long-dashed (blue), short-dashed (red), and dashed-dotted (gray) curves denote the total, u -, d -, and s -quark contributions to the internal force distributions, respectively.

4.4 Flavor-decomposed GFFs of the proton

We are now in a position to examine the t -dependence of the nucleon GFFs in the flavor SU(3) symmetry. By performing a 3D Fourier transform of the EMT distributions, we obtain the GFFs, which are depicted in Fig. 9. As discussed in the previous subsection, we have observed that the s -quark contributions to the A and J form factors are marginal. However, the s -quark's influences on the D and \bar{c} form factors are found to be non-negligible. Consequently, the s -quark plays an important role in the mechanical interpretation of the proton. For additional insights into the contributions of valence and sea quarks to the GFFs, refer to Ref. [141].

4.5 SU(3) spin-flavor structure and the hyperon GFFs

In the large N_c limit of QCD, the relation between the lowest-lying baryons can be understood in a model-independent manner using spin-flavor symmetry. While the GFFs in the flavor SU(2) symmetry were investigated in Ref. [104], we aim to extend this analysis to the flavor SU(3) sector in our current work. The chiral soliton approach describes the spin-flavor symmetry using collective operators, namely the spin S^i , isospin T^a , and spin-flavor D^{ia} generators. The matrix elements of these operators, which are listed in Tables 2 and 3, provide insights into the spin-flavor structure.

Utilizing the matrix elements of the spin-flavor operators, we establish the following spin-flavor relations in the flavor SU(3) symmetry:

- The flavor-singlet GFFs for the octet baryons are degenerate.
- The flavor-triplet GFFs are proportional to the isospin projection T_3 , i.e., $F_B^3 \propto T_3$. Consequently, we find the relations:

$$\sum_{B \in \text{octet}} F_B^3 = 0, \quad \sum_{B=p,n} F_B^3 = 0, \quad \sum_{B=\Sigma^+, \Sigma^0, \Sigma^-} F_B^3 = 0, \quad \sum_{B=\Xi^0, \Xi^-} F_B^3 = 0. \quad (4.32)$$

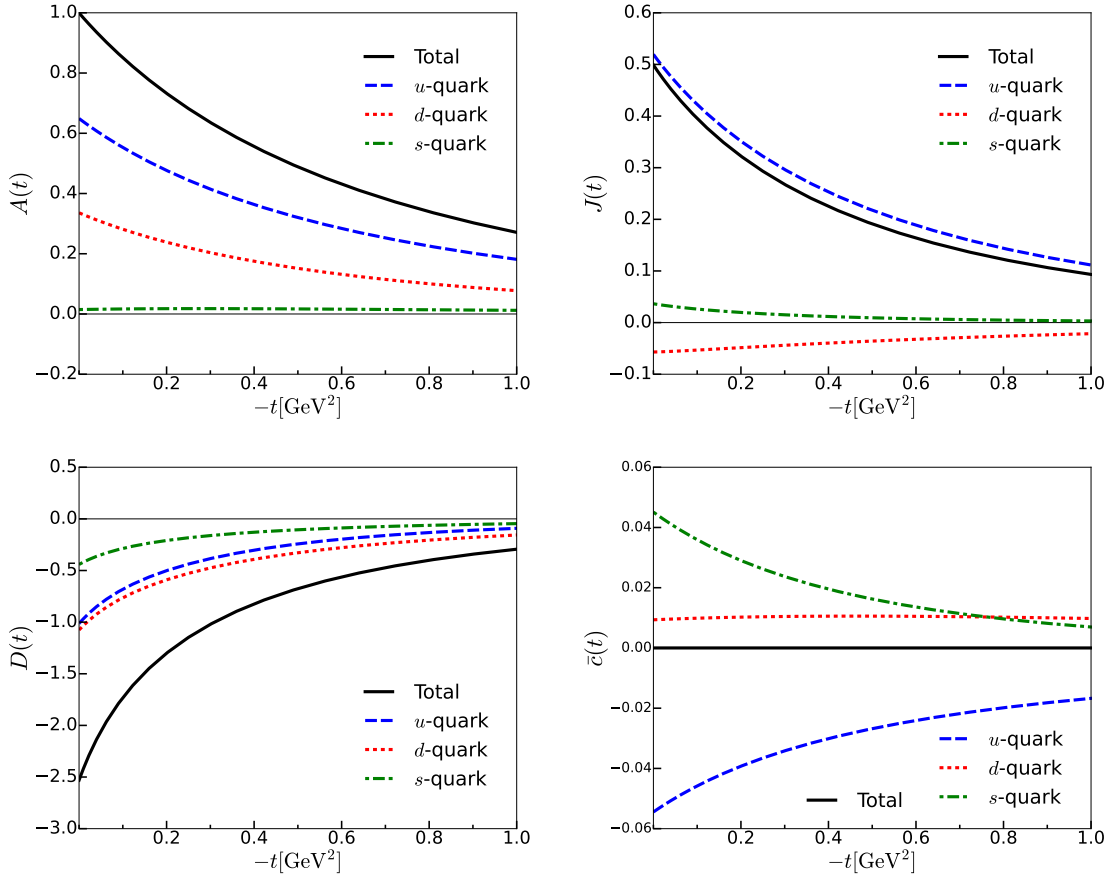


Figure 9. The gravitational form factors are drawn. The solid (black), long-dashed (blue), short-dashed (red), and dashed-dotted (green) curves denote the total, u -, d -, and s -quark contributions to the GFFs, respectively.

- The flavor-octet GFFs for the iso-multiplets are degenerate. Additionally, we obtain:

$$\sum_{B \in \text{octet}} F_B^8 = 0, \quad \sum_{B = \Lambda, \Sigma} F_B^8 = 0. \quad (4.33)$$

Remarkably, our numerical calculations confirm that these spin-flavor relations are indeed satisfied; see Tab. 1.

Figure 10 displays the $A^{0,3,8}$ form factors for the octet baryons. Firstly, we observe that the A^0 form factors for the octet baryons are clearly degenerate, which arises from the absence of m_s corrections. Introducing these corrections would break the degeneracy among the mass form factors A for the baryon octet, as discussed in Ref. [124]. Secondly, the A^3 form factors for the baryon octet are proportional to the third component of the isospin, denoted as $\propto T^3$. This implies that $A_{\Lambda^0, \Sigma^0}^3(t) = 0$. Additionally, the sums of the A^3 form factors for the iso-multiplets yield zero. Lastly, the A^8 form factors for the iso-multiplet

Table 1. Flavor-decomposed gravitational form factors for the octet baryons

B	$A_B^u(0)$	$A_B^d(0)$	$A_B^s(0)$	$J_B^u(0)$	$J_B^d(0)$	$J_B^s(0)$	$D_B^u(0)$	$D_B^d(0)$	$D_B^s(0)$	$\bar{c}_B^u(0)$	$\bar{c}_B^d(0)$	$\bar{c}_B^s(0)$
p	0.649	0.336	0.015	0.520	-0.057	0.036	-1.014	-1.076	-0.441	-0.054	0.009	0.045
n	0.336	0.649	0.015	-0.057	0.520	0.036	-1.076	-1.014	-0.441	0.009	-0.054	0.045
Λ	0.335	0.335	0.331	0.055	0.055	0.390	-0.960	-0.960	-0.611	0.005	0.005	-0.009
Σ^+	0.649	0.015	0.336	0.520	0.036	-0.057	-1.014	-0.441	-1.076	-0.054	0.045	0.009
Σ^0	0.332	0.332	0.336	0.278	0.278	-0.057	-0.727	-0.727	-1.076	-0.005	-0.005	0.009
Σ^-	0.015	0.649	0.336	0.036	0.520	-0.057	-0.441	-1.014	-1.076	0.045	-0.054	0.009
Ξ^0	0.336	0.015	0.649	-0.057	-0.036	0.552	-1.076	-0.441	-1.014	0.009	0.045	-0.054
Ξ^-	0.015	0.336	0.649	-0.036	-0.057	0.520	-0.441	-1.076	-1.014	0.045	0.009	-0.054

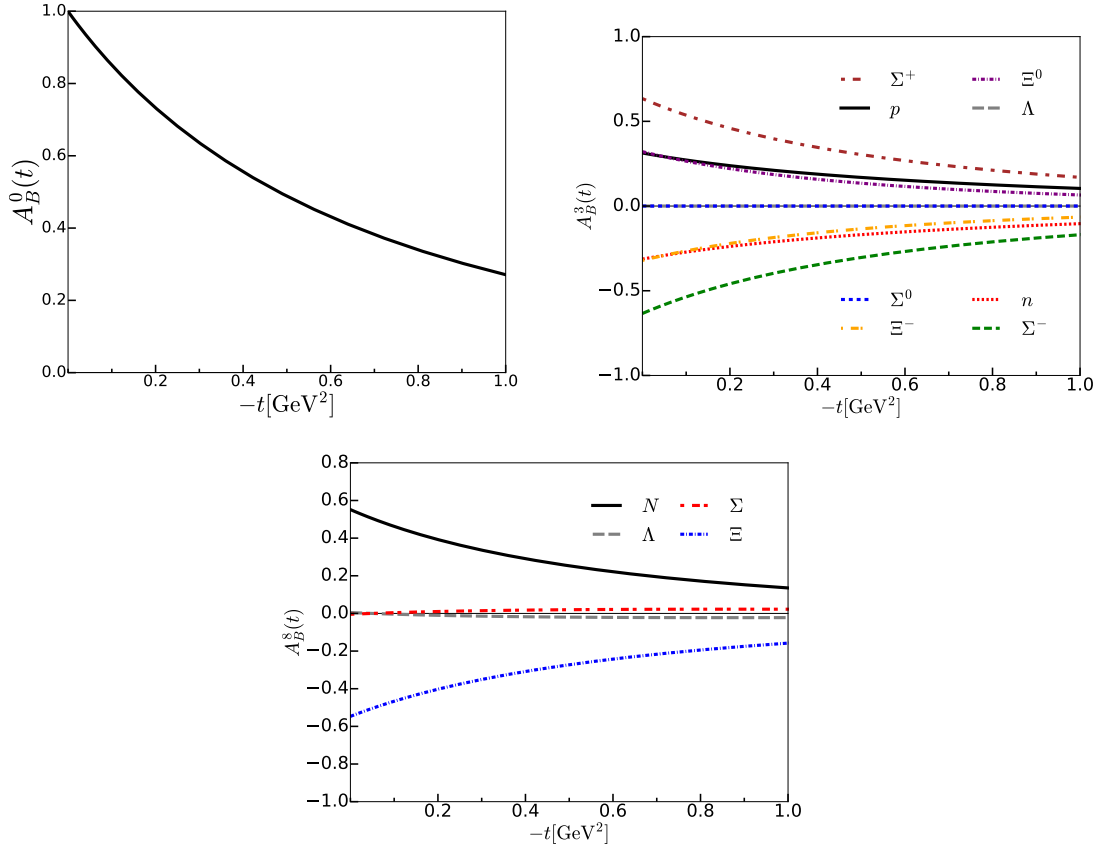


Figure 10. Flavor-singlet, -triplet, and -octet A form factors for the octet baryons are drawn.

members are degenerate. Interestingly, we derive the following relations:

$$\sum_{B=N,\Xi} A_B^8 = 0, \quad \sum_{B=\Lambda,\Sigma} A_B^8 = 0. \quad (4.34)$$

Consequently, Table 1 provides the flavor-decomposed GFFs. Notably, the u -, d -, and s -quarks equally carry the momentum fraction of the Λ^0 and Σ^0 baryons. This equality arises from the vanishing values of the flavor-octet components $A_{\Sigma^0,\Lambda^0}^8(0) = 0$. Comparing it with the proton, the Σ^+ baryon contains one less d -quark and one additional s -quark in the valence level, leading to an exchange in the roles of A^d and A^s between the proton and Σ^+ baryon. Similar tendencies are observed for the Σ^- , Ξ^0 , and Ξ^- baryons.

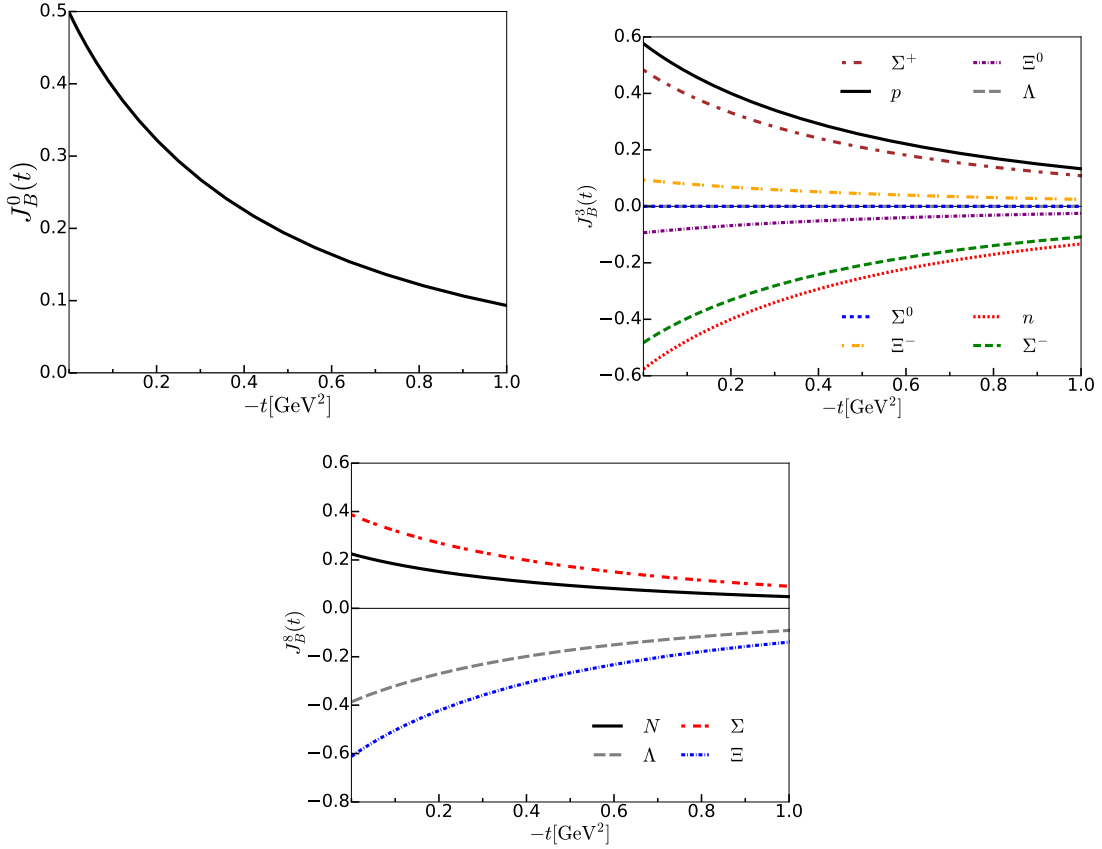


Figure 11. Flavor-singlet, -triplet, and -octet J form factors for the baryon octet are drawn.

Figure 11 illustrates the $J^{0,3,8}$ form factors for the octet baryons. Firstly, we observe that the J^0 form factors for the octet baryons are also degenerate. However, this degeneracy can be lifted by considering m_s corrections, as discussed in Ref. [124]. Secondly, the J^3 form factor for the octet baryons is once again proportional to T^3 , resulting in null results for the Σ^0 and Λ^0 baryons. While the octet components J^8 for the iso-multiplet members remain degenerate, we find the following relations:

$$\sum_{B=N,\Xi} J_B^8 \neq 0, \quad \sum_{B=\Lambda,\Sigma} J_B^8 = 0. \quad (4.35)$$

This is in contrast to the A^8 form factors, leading to different flavor-decomposed J form factors. In Table 1, we provide the flavor-decomposed J form factors. It is interesting to note that the Λ^0 and Σ^0 baryons exhibit different quark contributions despite having the same quark content. This finding is reminiscent of the flavor-decomposed axial charges presented in Ref. [147]:

$$\begin{aligned}\Delta u_{\Lambda^0} &= -0.093, & \Delta d_{\Lambda^0} &= -0.093, & \Delta s_{\Lambda^0} &= +0.623, \\ \Delta u_{\Sigma^0} &= +0.384, & \Delta d_{\Sigma^0} &= +0.384, & \Delta s_{\Sigma^0} &= -0.332.\end{aligned}\tag{4.36}$$

Thus, we conclude that the spin and OAM of the s -quark in the Λ^0 baryon are strongly polarized, while those in the Σ^0 baryon are relatively weakly polarized, despite both baryons having the same quark content. For the p , n , Σ^+ , Σ^- , Ξ^0 , and Ξ^- baryons, we can easily obtain the flavor-decomposed $J^q(0)$ form factors by considering the number of valence quarks. For instance, the flavor-decomposed $J^q(0)$ form factors for the Σ^+ baryon are found to be:

$$\begin{aligned}\text{two quarks with the same flavor } (u) &\rightarrow J^u(0) = +0.520, \\ \text{one quark } (s) &\rightarrow J^s(0) = -0.057, \\ \text{non-valence quark } (d) &\rightarrow J^d(0) = +0.036.\end{aligned}\tag{4.37}$$

In Fig. 12, we present the $D^{0,3,8}$ form factors for the octet baryons. We observe that the $D^0(t)$ form factors for the octet baryons are degenerate, similar to the previous cases. Additionally, the D^3 form factors for the octet baryons are proportional to T^3 , following the pattern we have seen before. Similarly to the J^8 form factor, the flavor-octet D^8 form factors for the iso-multiplet members are degenerate, leading to the following relations:

$$\sum_{B=N,\Xi} D_B^8 \neq 0, \quad \sum_{B=\Lambda,\Sigma} D_B^8 = 0.\tag{4.38}$$

Next, we investigate the flavor-decomposed D -term form factors. Interestingly, unlike the $J(t)$ form factors for the Λ^0 and Σ^0 baryons, we find that the s -quark contributions to the D -term for the Σ^0 baryon are larger than those for the Λ^0 baryon:

$$\begin{aligned}D_{\Lambda^0}^u &= -0.960, & D_{\Lambda^0}^d &= -0.960, & D_{\Lambda^0}^s &= -0.611, \\ D_{\Sigma^0}^u &= -0.727, & D_{\Sigma^0}^d &= -0.727, & D_{\Sigma^0}^s &= -1.076.\end{aligned}\tag{4.39}$$

Similarly, for the other octet baryons p , n , Σ^+ , Σ^- , Ξ^0 , and Ξ^- , we find that the flavor-decomposed D^q form factors can be obtained by counting the number of valence quarks. For example, the flavor-decomposed D -term form factors for the Σ^+ baryon are given by:

$$\begin{aligned}\text{two quarks with the same flavor } (u) &\rightarrow D^u(0) = -1.014, \\ \text{one quark } (s) &\rightarrow D^s(0) = -1.076, \\ \text{non-valence quark } (d) &\rightarrow D^d(0) = -0.441.\end{aligned}\tag{4.40}$$

These relations are exactly the same as the flavor-decomposed $J(t)$ form factors for the baryon octet. It is important to note that the contributions of non-valence quarks to the D -term form factors are rather significant. Therefore, these contributions should be considered

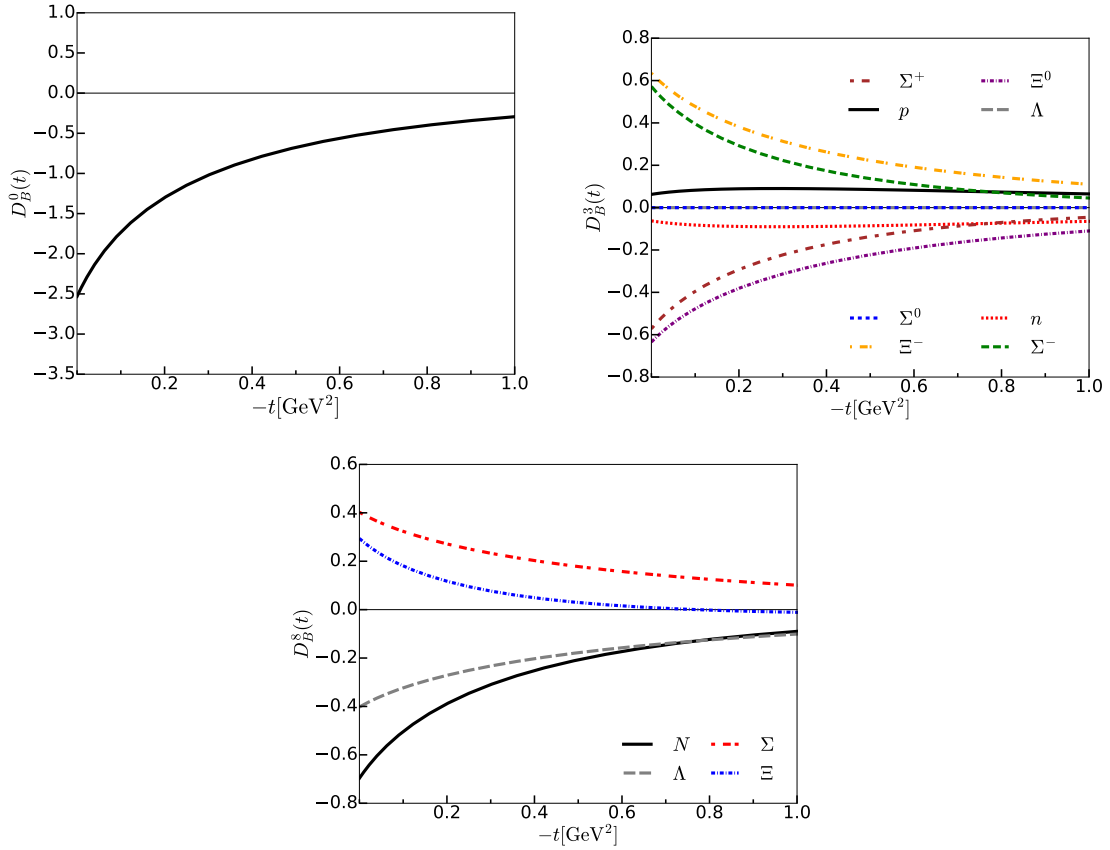


Figure 12. Flavor-singlet, -triplet, and -octet D -term form factors for the baryon octet are drawn.

in estimating the flavor-decomposed D -term form factors as they play an essential role alongside valence quarks.

In Fig. 13, we present the $\bar{c}^{0,3,8}$ form factors for the octet baryons. Remarkably, all the flavor-singlet, -triplet, and -octet \bar{c} form factors exhibit the same relations as the D -term form factors. When we perform the flavor decomposition of the \bar{c} form factor, we find the following relations:

$$\bar{c}_{\Lambda^0}^q(t) = -\bar{c}_{\Sigma^0}^q(t). \quad (4.41)$$

This result is attributed to the constraint imposed by the flavor-singlet $\bar{c}^0(t)$ form factor, namely $\bar{c}^0 = 0$. Additionally, we observe that the s -quark contributions to the \bar{c} form factors for the Λ^0 and Σ^0 baryons dominate over the u - and d -quark contributions:

$$\begin{aligned} \bar{c}_{\Lambda^0}^u &= +0.005, & \bar{c}_{\Lambda^0}^d &= +0.005, & \bar{c}_{\Lambda^0}^s &= -0.009, \\ \bar{c}_{\Sigma^0}^u &= -0.005, & \bar{c}_{\Sigma^0}^d &= -0.005, & \bar{c}_{\Sigma^0}^s &= +0.009. \end{aligned} \quad (4.42)$$

Similar relations hold for the other octet baryons, consistent with the findings for the flavor-decomposed $J(t)$ and $D(t)$ form factors. For instance, the flavor-decomposed \bar{c} form factors

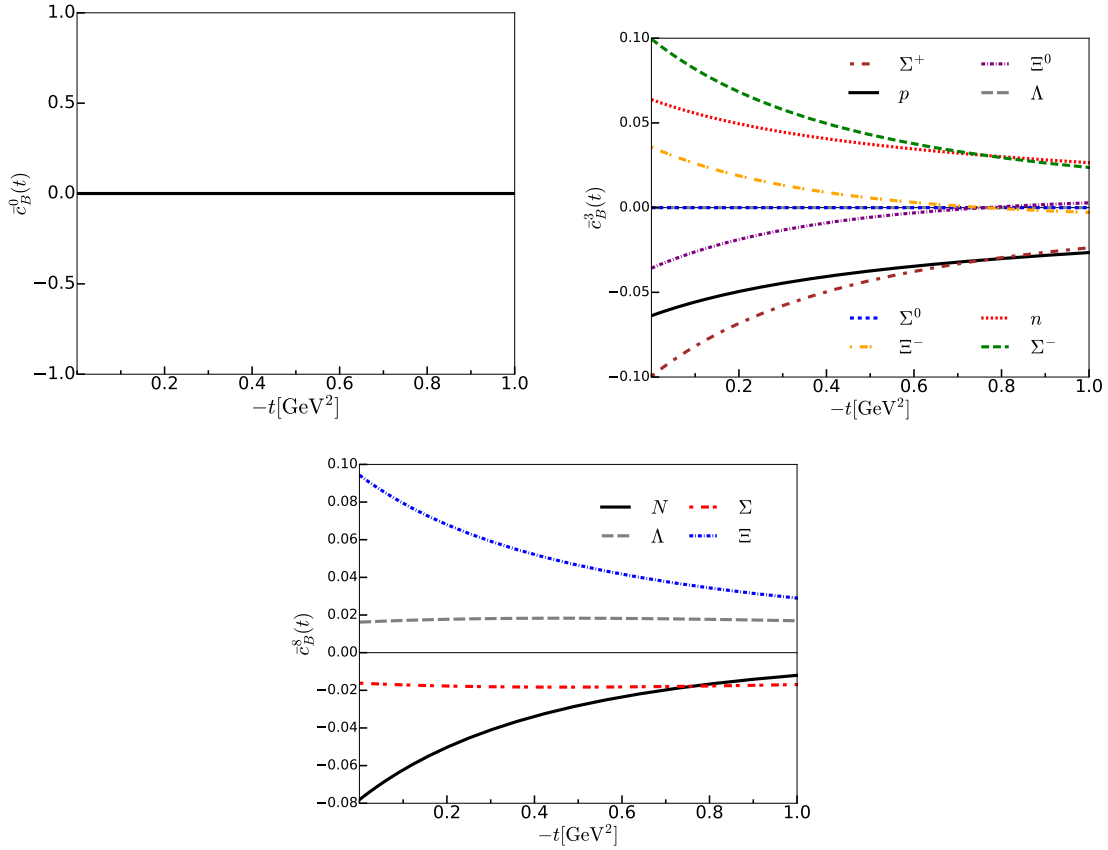


Figure 13. Flavor-singlet, -triplet, and -octet \bar{c} form factors for the octet baryons are drawn.

for the Σ^+ baryon are given by:

$$\begin{aligned}
 \text{two quarks with the same flavor } (u) &\rightarrow \bar{c}^u(0) = -0.054, \\
 \text{one quark } (s) &\rightarrow \bar{c}^s(0) = +0.009, \\
 \text{non-valence quark } (d) &\rightarrow \bar{c}^d(0) = +0.045.
 \end{aligned}
 \tag{4.43}$$

It is worth noting that the contributions of non-valence quarks turn out to be rather significant.

Finally, we turn our attention to the generalized electromagnetic form factors (GEMFFs). The first Mellin moments of the GPDs are directly related to the EMFFs. By retaining the flavor structure of the EMFFs, we can derive the GEMFFs through the second Mellin moments of the GPDs. The flavor structure of the electromagnetic current is given by the matrix:

$$Q = \begin{pmatrix} \frac{2}{3} & 0 & 0 \\ 0 & -\frac{1}{3} & 0 \\ 1 & 0 & -\frac{1}{3} \end{pmatrix} = \frac{1}{2} \left(\lambda^3 + \frac{1}{\sqrt{3}} \lambda^8 \right).
 \tag{4.44}$$

where λ^3 and λ^8 are Gell-Mann matrices. By inserting this flavor operator into the equation governing the electromagnetic current, Eq. (3.13), we obtain the GEMFFs. These GEMFFs

can be expressed as a linear combination of the flavor-triplet and -octet GFFs, namely $F_B^Q = \frac{1}{2} \left(F_B^3 + \frac{1}{\sqrt{3}} F_B^8 \right)$. Similar to the EMFFs, the GEMFFs satisfy the U -spin symmetry. This symmetry implies that the GEMFFs for baryons with the same charge, except for the Λ^0 and Σ^0 baryons, are equivalent when the flavor $SU(3)$ symmetry is imposed. In other words, we have:

$$F_p^Q(t) = F_{\Sigma^+}^Q(t), \quad F_n^Q(t) = F_{\Xi^0}^Q(t), \quad F_{\Sigma^-}^Q(t) = F_{\Xi^-}^Q(t), \quad F_{\Lambda^0}^Q(t) = -F_{\Sigma^0}^Q(t). \quad (4.45)$$

This U -spin symmetry is observed numerically in Fig. 14. The observed U -spin symmetry

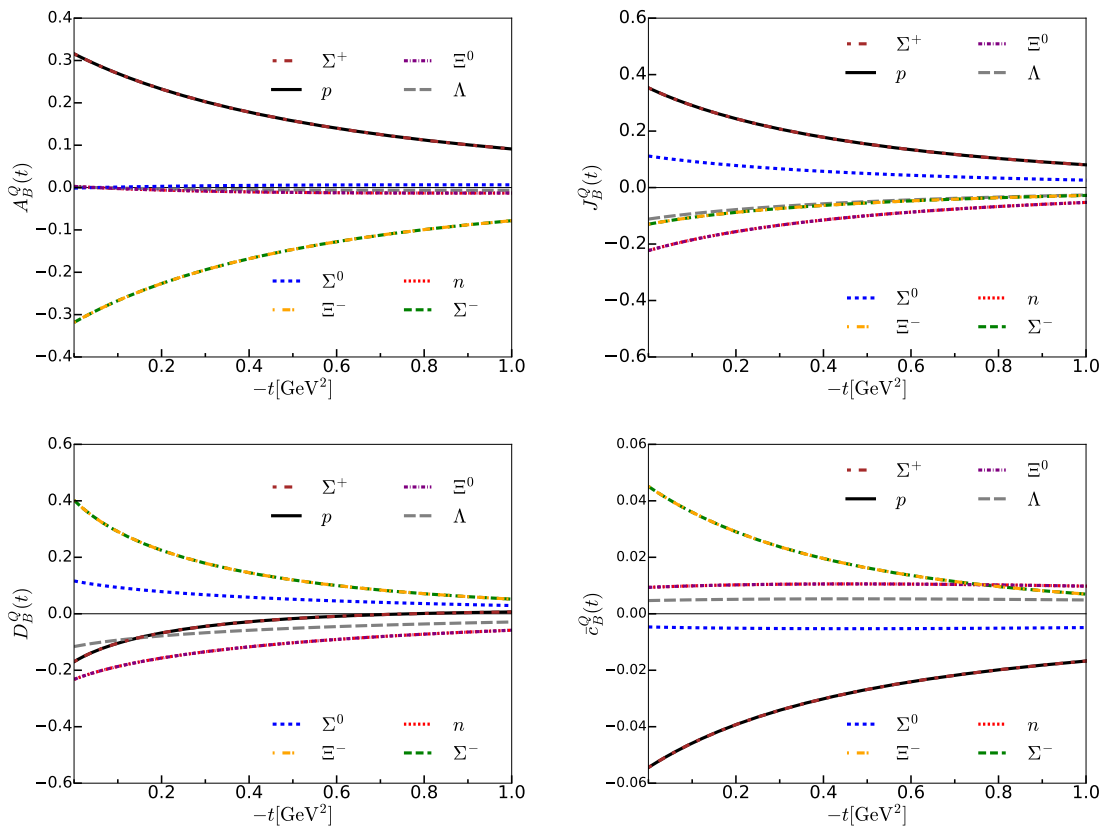


Figure 14. Generalized electromagnetic form factor for the octet baryons are drawn.

aligns with the spin-flavor relations found in the analysis of the separate flavor-singlet, -triplet, and -octet GFFs.

5 Conclusions and summary

In the current work, we focused on investigating the flavor-decomposed gravitational form factors (GFFs) for the nucleon and hyperons, and their mechanical interpretations within the framework of the $SU(3)$ chiral quark-soliton model. Specifically, we aimed to understand the role of the strange quark in the mechanics of the proton. In the large N_c limit

of quantum chromodynamics (QCD), the collective motion of the chiral soliton is nonrelativistic, while the internal dynamics remain fully relativistic. Therefore, we naturally adopt three-dimensional mechanical interpretations of the gravitational form factors.

Initially, we determined the large N_c behavior of the flavor-decomposed GFFs in the context of flavor SU(3) symmetry. The implementation of the trivial embedding of the SU(2) soliton into the SU(3) space led to modifications in the N_c behavior of the form factors. Notably, the N_c dependence of the flavor-triplet components of the A^3 , D^3 , and \bar{c}^3 form factors was enhanced by one order of N_c . As a consequence, all the flavor-singlet, -triplet, and -octet components of a form factor became parametrically equivalent. Conversely, the N_c behavior of the flavor-triplet J^3 form factor remained unchanged under flavor SU(3) symmetry, resulting in the continued suppression of the flavor-singlet J^0 form factor in the $1/N_c$ expansion.

Next, we obtained the flavor-decomposed mass distribution in the rest frame, which is influenced by both the A and \bar{c} form factors. While the flavor-singlet component was properly normalized to unity, i.e., $\sum_q (A^q(0) + \bar{c}^q(0)) = 1$, no constraints were imposed on the flavor-triplet and -octet components. Our findings revealed that approximately 60% of the proton mass is attributed to up quarks, 35% to down quarks, and 6% to strange quarks. Furthermore, the light-front momentum fraction carried by up, down, and strange quarks in the proton was estimated to be 65%, 34%, and 2%, respectively. Remarkably, this difference between mass decomposition and light-front momentum results from the contributions from the $\bar{c}^q(0)$ form factors.

Regarding the angular momentum distribution, we observed that the J form factor was appropriately normalized to the proton spin, i.e., $\sum_q J^q(0) = 1/2$. We determined the fraction of the proton spin carried by up, down, and strange quarks, which were found to be $J_p^u = 0.52$, $J_p^d = -0.06$, and $J_p^s = 0.04$, respectively. Similar to the mass form factor, the strange quark contributed minimally to the proton angular momentum. For the flavor-singlet angular momentum, it can be decomposed into orbital angular momentum and intrinsic quark spin, with each accounting for half of the proton spin. In this work, we focused on estimating the total angular momentum instead of the flavor-decomposed orbital angular momentum due to ambiguities in matching twist-3 QCD operators with the effective operators we employed.

Furthermore, we investigated the mechanical properties of the proton. The stress tensor was parameterized in terms of the pressure and shear-force distributions, which were obtained through three-dimensional Fourier transforms of the \bar{c} and D -term form factors. We verified that the von Laue condition, which corresponds to $\sum_q \bar{c}^q = 0$, was satisfied for the flavor-singlet pressure distribution. However, we discovered that the von Laue condition was violated for the flavor-triplet and -octet pressure distributions due to the contributions from the \bar{c} form factors. Additionally, we found no inherent relation between the shear force and pressure distributions through the differential equation derived from energy-momentum tensor current conservation. Notably, we observed that $D^{u-d} \sim 0$ was only valid in the flavor SU(3) symmetry, rather than the flavor SU(2). Moreover, in the flavor SU(3), we determined the significant contributions of strange quarks to the D -term and \bar{c} form factors. Using the Fourier transform of the obtained form factors, we visualize

these flavor-decomposed internal forces inside the proton, which revealed interplay between quark flavor subsystems.

Lastly, utilizing the spin-flavor symmetry in flavor SU(3) symmetry, we explored the GFFs for hyperons. We presented the interesting spin-flavor symmetries observed and introduced the electromagnetic flavor structure into the GFFs, resulting in the observation of U -spin symmetries in the generalized electromagnetic form factors.

6 Acknowledgement

The work was supported by the Basic Science Research Program through the National Research Foundation of Korea funded by the Korean government (Ministry of Education, Science and Technology, MEST), Grant-No. 2021R1A2C2093368 and 2018R1A5A1025563 (HYW and HChK). This work was also supported by the U.S. Department of Energy, Office of Science, Office of Nuclear Physics under contract DE-AC05-06OR23177 (JYK) and the the Ministère de l'Europe et des Affaires étrangères under scholarship 141295X (HYW).

A EMT distributions and regularization functions

We provide explicit expressions for the EMT distributions. These distributions are compiled below. We have mass distributions:

$$\begin{aligned}
\mathcal{E}(\mathbf{r}) &= N_c \left[E_v \psi_v^\dagger(\mathbf{r}) \psi_v(\mathbf{r}) + \sum_n \psi_n^\dagger(\mathbf{r}) \psi_n(\mathbf{r}) R_{0n} \right], \\
\mathcal{J}_1(\mathbf{r}) &= \frac{N_c}{4} \left[\sum_{n \neq v} \frac{E_n + E_v}{E_n - E_v} \langle n | \tau_3 | v \rangle \psi_v^\dagger(\mathbf{r}) \tau_3 \psi_n(\mathbf{r}) + \frac{1}{2} \sum_{n,m} (E_n + E_m) \langle n | \tau_3 | m \rangle \psi_m^\dagger(\mathbf{r}) \tau_3 \psi_n(\mathbf{r}) R_{3nm} \right], \\
\mathcal{J}_2(\mathbf{r}) &= \frac{N_c}{8} \left[\sum_{n^0} \frac{E_{n^0} + E_v}{E_{n^0} - E_v} \langle n^0 | v \rangle \psi_v^\dagger(\mathbf{r}) \psi_{n^0}(\mathbf{r}) \right. \\
&\quad \left. + \sum_{n^0, m} (E_{n^0} + E_m) \langle n^0 | m \rangle \psi_m^\dagger(\mathbf{r}) \psi_{n^0}(\mathbf{r}) R_{3n^0 m} \right], \tag{A.1}
\end{aligned}$$

and the angular momentum distributions:

$$\begin{aligned}
\mathcal{Q}_0(\mathbf{r}) &= \frac{N_c}{4} \left[\psi_v^\dagger(\mathbf{r}) \Gamma_{vv3}^J \tau_3 \psi_v(\mathbf{r}) - \frac{1}{2} \sum_n \text{sign}(E_n) \psi_n^\dagger(\mathbf{r}) \Gamma_{nn3}^J \tau_3 \psi_n(\mathbf{r}) \right], \\
\mathcal{Q}_1(\mathbf{r}) &= \frac{N_c}{4} i f_{ij3} \left[\sum_{n \neq v} \frac{\text{sign}(E_n)}{E_n - E_v} \langle n | \tau_i | v \rangle \psi_v^\dagger(\mathbf{r}) \tau_j \Gamma_{vn3}^J \psi_n(\mathbf{r}) \right. \\
&\quad \left. + \frac{1}{2} \sum_{n,m} \langle n | \tau_i | m \rangle \psi_m^\dagger(\mathbf{r}) \tau_j \Gamma_{mn3}^J \psi_n(\mathbf{r}) R_{6nm} \right], \\
\mathcal{I}_1(\mathbf{r}) &= \frac{N_c}{4} \left[\sum_{n \neq v} \frac{\langle n | \tau_3 | v \rangle}{E_n - E_v} \psi_v^\dagger(\mathbf{r}) \Gamma_{vn3}^J \psi_n(\mathbf{r}) + \frac{1}{2} \sum_{n,m} \langle n | \tau_3 | m \rangle \psi_m^\dagger(\mathbf{r}) \Gamma_{mn3}^J \psi_n(\mathbf{r}) R_{3nm} \right], \\
\mathcal{I}_2(\mathbf{r}) &= \frac{N_c}{4} \left[\sum_{n^0} \frac{\langle n^0 | v \rangle}{E_{n^0} - E_v} \psi_v^\dagger(\mathbf{r}) \tau_3 \Gamma_{vn^0 3}^J \psi_{n^0}(\mathbf{r}) \right. \\
&\quad \left. + \sum_{n^0, m} \langle n^0 | m \rangle \psi_m^\dagger(\mathbf{r}) \tau_3 \Gamma_{mn^0 3}^J \psi_{n^0}(\mathbf{r}) R_{3n^0 m} \right]. \tag{A.2}
\end{aligned}$$

where $\Gamma_3^J(E_n, E_m) = \Gamma_{nm3}^J = \left(2\hat{L}_3 + (E_n + E_m) \gamma_5 (\mathbf{r} \times \boldsymbol{\sigma})_3 \right)$ with $\hat{\mathbf{L}} = \left[\mathbf{r} \times \frac{i}{2} (\overleftarrow{\nabla} - \overrightarrow{\nabla}) \right]$. The quadrupole distributions $s(r)$ relevant for the D -term form factors are given by

$$\begin{aligned}
\mathcal{N}_1(\mathbf{r}) &= \frac{3}{2} N_c \left[\psi_v^\dagger(\mathbf{r}) \Gamma^s \psi_v(\mathbf{r}) + \sum_n \psi_n^\dagger(\mathbf{r}) \Gamma^s \psi_n(\mathbf{r}) R_{1n} \right], \\
\mathcal{J}_3(\mathbf{r}) &= \frac{3}{4} N_c \left[\sum_{n \neq v} \frac{\langle n | \tau_3 | v \rangle}{E_n - E_v} \psi_v^\dagger(\mathbf{r}) \tau_3 \Gamma^s \psi_n(\mathbf{r}) + \frac{1}{2} \sum_{n,m} \langle n | \tau_3 | m \rangle \psi_m^\dagger(\mathbf{r}) \tau_3 \Gamma^s \psi_n(\mathbf{r}) R_{5nm} \right], \\
\mathcal{J}_4(\mathbf{r}) &= \frac{3}{8} N_c \left[\sum_{n^0} \frac{\langle n^0 | v \rangle}{E_{n^0} - E_v} \psi_v^\dagger(\mathbf{r}) \Gamma^s \psi_{n^0}(\mathbf{r}) + \sum_{n^0, m} \langle n^0 | m \rangle \psi_m^\dagger(\mathbf{r}) \Gamma^s \psi_{n^0}(\mathbf{r}) R_{5n^0 m} \right], \tag{A.3}
\end{aligned}$$

and the monopole distributions $p(r)$ relevant to the \bar{c} and D -term form factors are written as

$$\begin{aligned}
\mathcal{N}_3(\mathbf{r}) &= \frac{N_c}{3} \left[\psi_v^\dagger(\mathbf{r}) \Gamma^p \psi_v(\mathbf{r}) + \sum_n \psi_n^\dagger(\mathbf{r}) \Gamma^p \psi_n(\mathbf{r}) R_{1n} \right], \\
\mathcal{J}_5(\mathbf{r}) &= \frac{N_c}{6} \left[\sum_{n \neq v} \frac{\langle n | \tau_3 | v \rangle}{E_n - E_v} \psi_v^\dagger(\mathbf{r}) \tau_3 \Gamma^p \psi_n(\mathbf{r}) + \frac{1}{2} \sum_{n,m} \langle n | \tau_3 | m \rangle \psi_m^\dagger(\mathbf{r}) \tau_3 \Gamma^p \psi_n(\mathbf{r}) R_{5nm} \right], \\
\mathcal{J}_6(\mathbf{r}) &= \frac{N_c}{12} \left[\sum_{n^0} \frac{\langle n^0 | v \rangle}{E_{n^0} - E_v} \psi_v^\dagger(\mathbf{r}) \Gamma^p \psi_{n^0}(\mathbf{r}) + \sum_{n^0, m} \langle n^0 | m \rangle \psi_m^\dagger(\mathbf{r}) \Gamma^p \psi_{n^0}(\mathbf{r}) R_{5n^0 m} \right], \tag{A.4}
\end{aligned}$$

where $\Gamma^s = \gamma^0 (\hat{\mathbf{n}} \cdot \mathbf{p}) - \frac{1}{3}\gamma^0 (\boldsymbol{\gamma} \cdot \mathbf{p})$ and $\Gamma^p = \gamma^0 (\boldsymbol{\gamma} \cdot \mathbf{p})$. The moments of inertia I_1 and I_2 are written as follows:

$$\begin{aligned}
I_1 &= \frac{N_c}{2} \left[\sum_{n \neq v} \frac{\langle n | \tau_3 | v \rangle}{E_n - E_v} \langle v | \tau_3 | n \rangle + \frac{1}{2} \sum_{n,m} \langle n | \tau_3 | m \rangle \langle m | \tau_3 | n \rangle R_{3nm} \right], \\
I_2 &= \frac{N_c}{4} \left[\sum_{n^0} \frac{\langle n^0 | v \rangle}{E_{n^0} - E_v} \psi_v^\dagger(\mathbf{r}) \psi_{n^0}(\mathbf{r}) + \sum_{n^0, m} \langle n^0 | m \rangle \psi_m^\dagger(\mathbf{r}) \psi_{n^0}(\mathbf{r}) R_{3n^0 m} \right]. \quad (\text{A.5})
\end{aligned}$$

In addition, all distributions are regularized, and their regularization functions are written as

$$\begin{aligned}
R_0(E_n) &:= R_{0n} = \frac{1}{4\sqrt{\pi}} \int_{\Lambda^{-2}} \frac{du}{u^{3/2}} e^{-uE_n^2}, \\
R_1(E_n) &:= R_{1n} = -\frac{E_n}{2\sqrt{\pi}} \int_{\Lambda^{-2}} \frac{du}{\sqrt{u}} e^{-uE_n^2}, \\
R_3(E_n, E_m) &:= R_{3nm} = \frac{1}{2\sqrt{\pi}} \int_{\Lambda^{-2}} \frac{du}{\sqrt{u}} \left[\frac{1}{u} \frac{e^{-uE_n^2} - e^{-uE_m^2}}{E_m^2 - E_n^2} - \frac{E_n e^{-uE_n^2} + E_m e^{-uE_m^2}}{E_n + E_m} \right], \\
R_5(E_n, E_m) &:= R_{5nm} = \frac{1}{2} \frac{\text{sign}(E_n) - \text{sign}(E_m)}{E_n - E_m}, \\
R_6(E_n, E_m) &:= R_{6nm} = \frac{1 - \text{sign}(E_n)\text{sign}(E_m)}{E_n - E_m}, \quad (\text{A.6})
\end{aligned}$$

with $\psi_v(\mathbf{r}) := \langle \mathbf{r} | v \rangle$ and $\psi_n(\mathbf{r}) := \langle \mathbf{r} | n \rangle$.

B Matrix elements of the spin-flavor operators

In Appendix B we list the matrix elements of the spin-flavor operators relevant to T^{00} and T^{ij} in Table 2, and those relevant to T^{0k} in Table 3.

Table 2. The matrix elements of the spin-flavor operators relevant to T^{00} and T^{ij} are listed.

B	Y	T	D_{38}	D_{88}	$D_{3i}J_i$	$D_{8i}J_i$	$D_{3a}J_a$	$D_{8a}J_a$
N	1	$\frac{1}{2}$	$\frac{\sqrt{3}}{15}T_3$	$\frac{3}{10}$	$-\frac{7}{10}T_3$	$-\frac{\sqrt{3}}{20}$	$-\frac{1}{5}T_3$	$-\frac{3\sqrt{3}}{10}$
Λ	0	0	0	$\frac{1}{10}$	0	$\frac{3\sqrt{3}}{20}$	0	$-\frac{\sqrt{3}}{10}$
Σ	0	1	$\frac{\sqrt{3}}{6}T_3$	$-\frac{1}{10}$	$-\frac{1}{4}T_3$	$-\frac{3\sqrt{3}}{20}$	$-\frac{1}{2}T_3$	$\frac{\sqrt{3}}{10}$
Ξ	-1	$\frac{1}{2}$	$\frac{4\sqrt{3}}{15}T_3$	$-\frac{1}{5}$	$\frac{1}{5}T_3$	$\frac{\sqrt{3}}{5}$	$-\frac{4}{5}T_3$	$\frac{\sqrt{3}}{5}$

Table 3. The matrix elements of the spin-flavor operators relevant to T^{0k} are listed.

B	Y	T	D_{33}	D_{83}	$D_{38}J_3$	$D_{88}J_3$	$d_{ab3}D_{3a}J_b$	$d_{ab3}D_{8a}J_b$
N	1	$\frac{1}{2}$	$-\frac{14}{15}T_3J_3$	$-\frac{\sqrt{3}}{15}J_3$	$\frac{\sqrt{3}}{15}T_3J_3$	$\frac{3}{10}J_3$	$\frac{7}{15}T_3J_3$	$\frac{\sqrt{3}}{30}J_3$
Λ	0	0	0	$\frac{\sqrt{3}}{5}J_3$	0	$\frac{1}{10}J_3$	0	$-\frac{\sqrt{3}}{10}J_3$
Σ	0	1	$-\frac{1}{3}T_3J_3$	$-\frac{\sqrt{3}}{5}J_3$	$\frac{\sqrt{3}}{6}T_3J_3$	$-\frac{1}{10}J_3$	$\frac{1}{6}T_3J_3$	$\frac{\sqrt{3}}{10}J_3$
Ξ	-1	$\frac{1}{2}$	$\frac{4}{15}T_3J_3$	$\frac{4\sqrt{3}}{15}J_3$	$\frac{4\sqrt{3}}{15}T_3J_3$	$-\frac{1}{5}J_3$	$-\frac{2}{15}T_3J_3$	$-\frac{2\sqrt{3}}{15}J_3$

References

- [1] EUROPEAN MUON collaboration, *A Measurement of the Spin Asymmetry and Determination of the Structure Function $g(1)$ in Deep Inelastic Muon-Proton Scattering*, *Phys. Lett. B* **206** (1988) 364.
- [2] EUROPEAN MUON collaboration, *An Investigation of the Spin Structure of the Proton in Deep Inelastic Scattering of Polarized Muons on Polarized Protons*, *Nucl. Phys. B* **328** (1989) 1.
- [3] C.A. Aidala, S.D. Bass, D. Hasch and G.K. Mallot, *The Spin Structure of the Nucleon*, *Rev. Mod. Phys.* **85** (2013) 655 [[1209.2803](#)].
- [4] D.B. Kaplan and A. Manohar, *Strange Matrix Elements in the Proton from Neutral Current Experiments*, *Nucl. Phys. B* **310** (1988) 527.
- [5] E.J. Beise, M.L. Pitt and D.T. Spayde, *The SAMPLE experiment and weak nucleon structure*, *Prog. Part. Nucl. Phys.* **54** (2005) 289 [[nucl-ex/0412054](#)].
- [6] A4 collaboration, *Measurement of strange quark contributions to the nucleon's form-factors at $Q^{*2} = 0.230$ -(GeV/c)**2*, *Phys. Rev. Lett.* **93** (2004) 022002 [[nucl-ex/0401019](#)].
- [7] F.E. Maas et al., *Evidence for strange quark contributions to the nucleon's form-factors at $q^{*2} = 0.108$ (GeV/c)**2*, *Phys. Rev. Lett.* **94** (2005) 152001 [[nucl-ex/0412030](#)].
- [8] HAPPEX collaboration, *Parity-violating electron scattering from He-4 and the strange electric form-factor of the nucleon*, *Phys. Rev. Lett.* **96** (2006) 022003 [[nucl-ex/0506010](#)].
- [9] G0 collaboration, *Strange quark contributions to parity-violating asymmetries in the forward G0 electron-proton scattering experiment*, *Phys. Rev. Lett.* **95** (2005) 092001 [[nucl-ex/0506021](#)].
- [10] G0 collaboration, *Strange Quark Contributions to Parity-Violating Asymmetries in the Backward Angle G0 Electron Scattering Experiment*, *Phys. Rev. Lett.* **104** (2010) 012001 [[0909.5107](#)].
- [11] F.E. Maas and K.D. Paschke, *Strange nucleon form-factors*, *Prog. Part. Nucl. Phys.* **95** (2017) 209.

- [12] B. Borasoy and U.-G. Meissner, *Chiral Expansion of Baryon Masses and σ -Terms*, *Annals Phys.* **254** (1997) 192 [[hep-ph/9607432](#)].
- [13] H.-C. Kim, M.V. Polyakov and K. Goeke, *Tensor charges of the nucleon in the $SU(3)$ chiral quark soliton model*, *Phys. Lett. B* **387** (1996) 577 [[hep-ph/9604442](#)].
- [14] T. Ledwig, A. Silva and H.-C. Kim, *Tensor charges and form factors of $SU(3)$ baryons in the self-consistent $SU(3)$ chiral quark-soliton model*, *Phys. Rev. D* **82** (2010) 034022 [[1004.3612](#)].
- [15] I.Y. Kobzarev and L.B. Okun, *GRAVITATIONAL INTERACTION OF FERMIONS*, *Zh. Eksp. Teor. Fiz.* **43** (1962) 1904.
- [16] H. Pagels, *Energy-Momentum Structure Form Factors of Particles*, *Phys. Rev.* **144** (1966) 1250.
- [17] X.-D. Ji, *Gauge-Invariant Decomposition of Nucleon Spin*, *Phys. Rev. Lett.* **78** (1997) 610 [[hep-ph/9603249](#)].
- [18] M.V. Polyakov, *Generalized parton distributions and strong forces inside nucleons and nuclei*, *Phys. Lett. B* **555** (2003) 57 [[hep-ph/0210165](#)].
- [19] D. Müller, D. Robaschik, B. Geyer, F.M. Dittes and J. Hořejši, *Wave functions, evolution equations and evolution kernels from light ray operators of QCD*, *Fortsch. Phys.* **42** (1994) 101 [[hep-ph/9812448](#)].
- [20] X.-D. Ji, *Deeply virtual Compton scattering*, *Phys. Rev. D* **55** (1997) 7114 [[hep-ph/9609381](#)].
- [21] A.V. Radyushkin, *Scaling limit of deeply virtual Compton scattering*, *Phys. Lett. B* **380** (1996) 417 [[hep-ph/9604317](#)].
- [22] A.V. Radyushkin, *Asymmetric gluon distributions and hard diffractive electroproduction*, *Phys. Lett. B* **385** (1996) 333 [[hep-ph/9605431](#)].
- [23] C. Lorcé, *On the hadron mass decomposition*, *Eur. Phys. J. C* **78** (2018) 120 [[1706.05853](#)].
- [24] C. Lorcé, A. Metz, B. Pasquini and S. Rodini, *Energy-momentum tensor in QCD: nucleon mass decomposition and mechanical equilibrium*, *JHEP* **11** (2021) 121 [[2109.11785](#)].
- [25] M.A. Shifman, A.I. Vainshtein and V.I. Zakharov, *Remarks on Higgs Boson Interactions with Nucleons*, *Phys. Lett. B* **78** (1978) 443.
- [26] X.-D. Ji, *A QCD analysis of the mass structure of the nucleon*, *Phys. Rev. Lett.* **74** (1995) 1071 [[hep-ph/9410274](#)].
- [27] X.-D. Ji, *Breakup of hadron masses and energy - momentum tensor of QCD*, *Phys. Rev. D* **52** (1995) 271 [[hep-ph/9502213](#)].
- [28] Y.-B. Yang, J. Liang, Y.-J. Bi, Y. Chen, T. Draper, K.-F. Liu et al., *Proton Mass Decomposition from the QCD Energy Momentum Tensor*, *Phys. Rev. Lett.* **121** (2018) 212001 [[1808.08677](#)].
- [29] A. Metz, B. Pasquini and S. Rodini, *Revisiting the proton mass decomposition*, *Phys. Rev. D* **102** (2020) 114042 [[2006.11171](#)].
- [30] I. Zahed, *Mass sum rule of hadrons in the QCD instanton vacuum*, *Phys. Rev. D* **104** (2021) 054031 [[2102.08191](#)].

- [31] X. Ji, *Proton mass decomposition: naturalness and interpretations*, *Front. Phys. (Beijing)* **16** (2021) 64601 [[2102.07830](#)].
- [32] K.-F. Liu, *Proton mass decomposition and hadron cosmological constant*, *Phys. Rev. D* **104** (2021) 076010 [[2103.15768](#)].
- [33] E. Leader and C. Lorcé, *The angular momentum controversy: What's it all about and does it matter?*, *Phys. Rept.* **541** (2014) 163 [[1309.4235](#)].
- [34] E. Leader, *A critical assessment of the angular momentum sum rules*, *Phys. Lett. B* **720** (2013) 120 [[1211.3957](#)].
- [35] NEW MUON collaboration, *The Gottfried sum from the ratio $F_2(n) / F_2(p)$* , *Phys. Rev. Lett.* **66** (1991) 2712.
- [36] NEW MUON collaboration, *Accurate measurement of $F_2(d) / F_2(p)$ and $R^{*d} - R^{*p}$* , *Nucl. Phys. B* **487** (1997) 3 [[hep-ex/9611022](#)].
- [37] HERMES collaboration, *The Flavor asymmetry of the light quark sea from semiinclusive deep inelastic scattering*, *Phys. Rev. Lett.* **81** (1998) 5519 [[hep-ex/9807013](#)].
- [38] NUSEA collaboration, *Improved measurement of the anti-d / anti-u asymmetry in the nucleon sea*, *Phys. Rev. D* **64** (2001) 052002 [[hep-ex/0103030](#)].
- [39] F. Belinfante, *On the spin angular momentum of mesons*, *Physica* **6** (1939) 887.
- [40] L. Rosenfeld, *On the energy-momentum tensor*, *Mém. Acad. Roy. Belg* **18** (1940) .
- [41] A.V. Belitsky and A.V. Radyushkin, *Unraveling hadron structure with generalized parton distributions*, *Phys. Rept.* **418** (2005) 1 [[hep-ph/0504030](#)].
- [42] C. Lorcé, L. Mantovani and B. Pasquini, *Spatial distribution of angular momentum inside the nucleon*, *Phys. Lett. B* **776** (2018) 38 [[1704.08557](#)].
- [43] P. Schweitzer and K. Tezgin, *Monopole and quadrupole contributions to the angular momentum density*, *Phys. Lett. B* **796** (2019) 47 [[1905.12336](#)].
- [44] SPIN MUON collaboration, *Measurement of the spin dependent structure function $g_1(x)$ of the deuteron*, *Phys. Lett. B* **302** (1993) 533.
- [45] E142 collaboration, *Determination of the neutron spin structure function.*, *Phys. Rev. Lett.* **71** (1993) 959.
- [46] J.R. Ellis and M. Karliner, *Analysis of data on polarized lepton - nucleon scattering*, *Phys. Lett. B* **313** (1993) 131 [[hep-ph/9305306](#)].
- [47] SPIN MUON (SMC) collaboration, *Polarization of valence and nonstrange sea quarks in the nucleon from semiinclusive spin asymmetries*, *Phys. Lett. B* **369** (1996) 93.
- [48] SPIN MUON collaboration, *Polarized quark distributions in the nucleon from semiinclusive spin asymmetries*, *Phys. Lett. B* **420** (1998) 180 [[hep-ex/9711008](#)].
- [49] HERMES collaboration, *Flavor decomposition of the sea quark helicity distributions in the nucleon from semiinclusive deep inelastic scattering*, *Phys. Rev. Lett.* **92** (2004) 012005 [[hep-ex/0307064](#)].
- [50] HERMES collaboration, *Quark helicity distributions in the nucleon for up, down, and strange quarks from semi-inclusive deep-inelastic scattering*, *Phys. Rev. D* **71** (2005) 012003 [[hep-ex/0407032](#)].

- [51] COMPASS collaboration, *The Deuteron Spin-dependent Structure Function $g_1(d)$ and its First Moment*, *Phys. Lett. B* **647** (2007) 8 [[hep-ex/0609038](#)].
- [52] COMPASS collaboration, *The Spin-dependent Structure Function of the Proton g_1^p and a Test of the Bjorken Sum Rule*, *Phys. Lett. B* **690** (2010) 466 [[1001.4654](#)].
- [53] PARTICLE DATA GROUP collaboration, *Review of Particle Physics*, *PTEP* **2022** (2022) 083C01.
- [54] F.E. Close and R.G. Roberts, *Consistent analysis of the spin content of the nucleon*, *Phys. Lett. B* **316** (1993) 165 [[hep-ph/9306289](#)].
- [55] J.R. Ellis and R.L. Jaffe, *A Sum Rule for Deep Inelastic Electroproduction from Polarized Protons*, *Phys. Rev. D* **9** (1974) 1444.
- [56] S.D. Bass, *The Spin structure of the proton*, *Rev. Mod. Phys.* **77** (2005) 1257 [[hep-ph/0411005](#)].
- [57] LHPC collaboration, *Nucleon structure from mixed action calculations using 2+1 flavors of asqtad sea and domain wall valence fermions*, *Phys. Rev. D* **82** (2010) 094502 [[1001.3620](#)].
- [58] QCDSF collaboration, *Generalized parton distributions from lattice QCD*, *Phys. Rev. Lett.* **92** (2004) 042002 [[hep-ph/0304249](#)].
- [59] LHPC collaboration, *Nucleon Generalized Parton Distributions from Full Lattice QCD*, *Phys. Rev. D* **77** (2008) 094502 [[0705.4295](#)].
- [60] G.S. Bali, S. Collins, M. Göckeler, R. Rödl, A. Schäfer and A. Sternbeck, *Nucleon generalized form factors from two-flavor lattice QCD*, *Phys. Rev. D* **100** (2019) 014507 [[1812.08256](#)].
- [61] C. Alexandrou et al., *Moments of nucleon generalized parton distributions from lattice QCD simulations at physical pion mass*, *Phys. Rev. D* **101** (2020) 034519 [[1908.10706](#)].
- [62] M. Penttinen, M.V. Polyakov, A.G. Shuvaev and M. Strikman, *DVCS amplitude in the parton model*, *Phys. Lett. B* **491** (2000) 96 [[hep-ph/0006321](#)].
- [63] Y. Hatta and S. Yoshida, *Twist analysis of the nucleon spin in QCD*, *JHEP* **10** (2012) 080 [[1207.5332](#)].
- [64] X. Ji, X. Xiong and F. Yuan, *Probing Parton Orbital Angular Momentum in Longitudinally Polarized Nucleon*, *Phys. Rev. D* **88** (2013) 014041 [[1207.5221](#)].
- [65] M.V. Polyakov and C. Weiss, *Skewed and double distributions in pion and nucleon*, *Phys. Rev. D* **60** (1999) 114017 [[hep-ph/9902451](#)].
- [66] P. Schweitzer, S. Boffi and M. Radici, *Polynomiality of unpolarized off forward distribution functions and the D term in the chiral quark soliton model*, *Phys. Rev. D* **66** (2002) 114004 [[hep-ph/0207230](#)].
- [67] C. Cebulla, K. Goeke, J. Ossmann and P. Schweitzer, *The Nucleon form-factors of the energy momentum tensor in the Skyrme model*, *Nucl. Phys. A* **794** (2007) 87 [[hep-ph/0703025](#)].
- [68] K. Goeke, J. Grabis, J. Ossmann, M.V. Polyakov, P. Schweitzer, A. Silva et al., *Nucleon form-factors of the energy momentum tensor in the chiral quark-soliton model*, *Phys. Rev. D* **75** (2007) 094021 [[hep-ph/0702030](#)].
- [69] M. Wakamatsu, *On the D-term of the nucleon generalized parton distributions*, *Phys. Lett. B* **648** (2007) 181 [[hep-ph/0701057](#)].

- [70] K. Kumerički, *Measurability of pressure inside the proton*, *Nature* **570** (2019) E1.
- [71] V.D. Burkert, L. Elouadrhiri and F.X. Girod, *The pressure distribution inside the proton*, *Nature* **557** (2018) 396.
- [72] V.D. Burkert, L. Elouadrhiri and F.X. Girod, *Determination of shear forces inside the proton*, [2104.02031](#).
- [73] M.V. Polyakov and P. Schweitzer, *Forces inside hadrons: pressure, surface tension, mechanical radius, and all that*, *Int. J. Mod. Phys. A* **33** (2018) 1830025 [[1805.06596](#)].
- [74] C. Lorcé, H. Moutarde and A.P. Trawiński, *Revisiting the mechanical properties of the nucleon*, *Eur. Phys. J. C* **79** (2019) 89 [[1810.09837](#)].
- [75] V.D. Burkert, L. Elouadrhiri, F.X. Girod, C. Lorcé, P. Schweitzer and P.E. Shanahan, *Colloquium: Gravitational Form Factors of the Proton*, [2303.08347](#).
- [76] Y. Hatta and M. Strikman, *ϕ -meson lepto-production near threshold and the strangeness D -term*, *Phys. Lett. B* **817** (2021) 136295 [[2102.12631](#)].
- [77] E. Witten, *Baryons in the $1/n$ Expansion*, *Nucl. Phys. B* **160** (1979) 57.
- [78] E. Witten, *Current Algebra, Baryons, and Quark Confinement*, *Nucl. Phys. B* **223** (1983) 433.
- [79] R.F. Dashen and A.V. Manohar, *Baryon - pion couplings from large $N(c)$ QCD*, *Phys. Lett. B* **315** (1993) 425 [[hep-ph/9307241](#)].
- [80] R.F. Dashen, E.E. Jenkins and A.V. Manohar, *The $1/N(c)$ expansion for baryons*, *Phys. Rev. D* **49** (1994) 4713 [[hep-ph/9310379](#)].
- [81] R.F. Dashen, E.E. Jenkins and A.V. Manohar, *Spin flavor structure of large $N(c)$ baryons*, *Phys. Rev. D* **51** (1995) 3697 [[hep-ph/9411234](#)].
- [82] D. Diakonov and V.Y. Petrov, *A Theory of Light Quarks in the Instanton Vacuum*, *Nucl. Phys. B* **272** (1986) 457.
- [83] D. Diakonov, *Instantons at work*, *Prog. Part. Nucl. Phys.* **51** (2003) 173 [[hep-ph/0212026](#)].
- [84] A. Blotz, M. Praszalowicz and K. Goeke, *Gottfried sum in the $SU(3)$ NJL model*, *Phys. Rev. D* **53** (1996) 551.
- [85] P.V. Pobylitsa, M.V. Polyakov, K. Goeke, T. Watabe and C. Weiss, *Isovector unpolarized quark distribution in the nucleon in the large $N(c)$ limit*, *Phys. Rev. D* **59** (1999) 034024 [[hep-ph/9804436](#)].
- [86] D. Diakonov, V. Petrov, P. Pobylitsa, M.V. Polyakov and C. Weiss, *Nucleon parton distributions at low normalization point in the large $N(c)$ limit*, *Nucl. Phys. B* **480** (1996) 341 [[hep-ph/9606314](#)].
- [87] D. Diakonov, V.Y. Petrov, P.V. Pobylitsa, M.V. Polyakov and C. Weiss, *Unpolarized and polarized quark distributions in the large $N(c)$ limit*, *Phys. Rev. D* **56** (1997) 4069 [[hep-ph/9703420](#)].
- [88] M. Wakamatsu and T. Kubota, *Chiral symmetry and the nucleon spin structure functions*, *Phys. Rev. D* **60** (1999) 034020 [[hep-ph/9809443](#)].
- [89] H.-C. Kim, M.V. Polyakov and K. Goeke, *Nucleon tensor charges in the $SU(2)$ chiral quark - soliton model*, *Phys. Rev. D* **53** (1996) 4715 [[hep-ph/9509283](#)].

- [90] P. Schweitzer, D. Urbano, M.V. Polyakov, C. Weiss, P.V. Pobylitsa and K. Goeke, *Transversity distributions in the nucleon in the large $N(c)$ limit*, *Phys. Rev. D* **64** (2001) 034013 [[hep-ph/0101300](#)].
- [91] M. Wakamatsu, *Chiral odd distribution functions in the chiral quark soliton model*, *Phys. Lett. B* **509** (2001) 59 [[hep-ph/0012331](#)].
- [92] A. Blotz, M.V. Polyakov and K. Goeke, *The Spin of the proton in the solitonic $SU(3)$ NJL model*, *Phys. Lett. B* **302** (1993) 151.
- [93] A. Blotz, M. Praszalowicz and K. Goeke, *Axial properties of the nucleon with $1/N(c)$ corrections in the solitonic $SU(3)$ NJL model*, *Phys. Rev. D* **53** (1996) 485 [[hep-ph/9403314](#)].
- [94] H.-C. Kim, A. Blotz, C. Schneider and K. Goeke, *Strangeness in the scalar form-factor of the nucleon*, *Nucl. Phys. A* **596** (1996) 415 [[hep-ph/9508299](#)].
- [95] A. Silva, H.-C. Kim and K. Goeke, *Strange form-factors in the context of SAMPLE, HAPPEX, and A_4 experiments*, *Phys. Rev. D* **65** (2002) 014016 [[hep-ph/0107185](#)].
- [96] C.V. Christov, A. Blotz, H.-C. Kim, P. Pobylitsa, T. Watabe, T. Meissner et al., *Baryons as nontopological chiral solitons*, *Prog. Part. Nucl. Phys.* **37** (1996) 91 [[hep-ph/9604441](#)].
- [97] M. Wakamatsu and H. Yoshiki, *A Chiral quark model of the nucleon*, *Nucl. Phys. A* **524** (1991) 561.
- [98] D.R. Yennie, M.M. Lévy and D.G. Ravenhall, *Electromagnetic structure of nucleons*, *Rev. Mod. Phys.* **29** (1957) 144.
- [99] M. Burkardt, *Impact parameter dependent parton distributions and off forward parton distributions for zeta $\rightarrow 0$* , *Phys. Rev. D* **62** (2000) 071503 [[hep-ph/0005108](#)].
- [100] M. Burkardt, *Impact parameter space interpretation for generalized parton distributions*, *Int. J. Mod. Phys. A* **18** (2003) 173 [[hep-ph/0207047](#)].
- [101] G.A. Miller, *Charge Density of the Neutron*, *Phys. Rev. Lett.* **99** (2007) 112001 [[0705.2409](#)].
- [102] R.L. Jaffe, *Ambiguities in the definition of local spatial densities in light hadrons*, *Phys. Rev. D* **103** (2021) 016017 [[2010.15887](#)].
- [103] C. Lorcé, P. Schweitzer and K. Tezgin, *2D energy-momentum tensor distributions of nucleon in a large- N_c quark model from ultrarelativistic to nonrelativistic limit*, *Phys. Rev. D* **106** (2022) 014012 [[2202.01192](#)].
- [104] J.-Y. Kim, H.-Y. Won, J.L. Goity and C. Weiss, *QCD angular momentum in $N \rightarrow \Delta$ transitions*, [2304.08575](#).
- [105] I.Y. Kobsarev and V.I. Zakharov, *Consequences of the transversality of the graviton emission amplitude*, *Annals Phys.* **60** (1970) 448.
- [106] K.L. Ng, *Gravitational form-factors of the neutrino*, *Phys. Rev. D* **47** (1993) 5187 [[gr-qc/9305002](#)].
- [107] S. Cotogno, C. Lorcé, P. Lowdon and M. Morales, *Covariant multipole expansion of local currents for massive states of any spin*, *Phys. Rev. D* **101** (2020) 056016 [[1912.08749](#)].
- [108] J.-Y. Kim, *Parametrization of transition energy-momentum tensor form factors*, *Phys. Lett. B* **834** (2022) 137442 [[2206.10202](#)].

- [109] G.A. Miller, *Transverse Charge Densities*, *Ann. Rev. Nucl. Part. Sci.* **60** (2010) 1 [1002.0355].
- [110] R.G. Sachs, *High-Energy Behavior of Nucleon Electromagnetic Form Factors*, *Phys. Rev.* **126** (1962) 2256.
- [111] C. Lorcé, *Charge Distributions of Moving Nucleons*, *Phys. Rev. Lett.* **125** (2020) 232002 [2007.05318].
- [112] Y. Chen and C. Lorcé, *Nucleon relativistic polarization and magnetization distributions*, **2302.04672**.
- [113] C. Lorcé and P. Wang, *Deuteron relativistic charge distributions*, *Phys. Rev. D* **105** (2022) 096032 [2204.01465].
- [114] Y. Chen and C. Lorcé, *Pion and nucleon relativistic electromagnetic four-current distributions*, *Phys. Rev. D* **106** (2022) 116024 [2210.02908].
- [115] E. Epelbaum, J. Gegelia, N. Lange, U.G. Meißner and M.V. Polyakov, *Definition of Local Spatial Densities in Hadrons*, *Phys. Rev. Lett.* **129** (2022) 012001 [2201.02565].
- [116] J.Y. Panteleeva, E. Epelbaum, J. Gegelia and U.G. Meißner, *Definition of electromagnetic local spatial densities for composite spin-1/2 systems*, *Phys. Rev. D* **106** (2022) 056019 [2205.15061].
- [117] H. Alharazin, B.D. Sun, E. Epelbaum, J. Gegelia and U.G. Meißner, *Local spatial densities for composite spin-3/2 systems*, *JHEP* **02** (2023) 163 [2212.11505].
- [118] M.V. Polyakov and H.-D. Son, *Nucleon gravitational form factors from instantons: forces between quark and gluon subsystems*, *JHEP* **09** (2018) 156 [1808.00155].
- [119] H.-Y. Won, H.-C. Kim and J.-Y. Kim, *Nucleon cosmological constant term and flavor structure of the gravitational form factors*, **2302.02974**.
- [120] I.A. Perevalova, M.V. Polyakov and P. Schweitzer, *On LHCb pentaquarks as a baryon- $\psi(2S)$ bound state: prediction of isospin- $\frac{3}{2}$ pentaquarks with hidden charm*, *Phys. Rev. D* **94** (2016) 054024 [1607.07008].
- [121] M.V. Polyakov and P. Schweitzer, *Mechanical properties of particles*, *PoS SPIN2018* (2019) 066 [1812.06143].
- [122] K. Goeke, J. Ossmann, P. Schweitzer and A. Silva, *Pion mass dependence of the nucleon mass and chiral extrapolation of lattice data in the chiral quark soliton model*, *Eur. Phys. J. A* **27** (2006) 77 [hep-lat/0505010].
- [123] B.L. Ioffe, *Calculation of Baryon Masses in Quantum Chromodynamics*, *Nucl. Phys. B* **188** (1981) 317.
- [124] H.-Y. Won, J.-Y. Kim and H.-C. Kim, *Gravitational form factors of the baryon octet with flavor $SU(3)$ symmetry breaking*, *Phys. Rev. D* **106** (2022) 114009 [2210.03320].
- [125] J.Y. Panteleeva and M.V. Polyakov, *Quadrupole pressure and shear forces inside baryons in the large N_c limit*, *Phys. Lett. B* **809** (2020) 135707 [2004.02912].
- [126] J.-Y. Kim and B.-D. Sun, *Gravitational form factors of a baryon with spin-3/2*, *Eur. Phys. J. C* **81** (2021) 85 [2011.00292].
- [127] J. Balla, M.V. Polyakov and C. Weiss, *Nucleon matrix elements of higher twist operators from the instanton vacuum*, *Nucl. Phys. B* **510** (1998) 327 [hep-ph/9707515].

- [128] K. Goeke, J. Grabis, J. Ossmann, P. Schweitzer, A. Silva and D. Urbano, *The pion mass dependence of the nucleon form-factors of the energy momentum tensor in the chiral quark-soliton model*, *Phys. Rev. C* **75** (2007) 055207 [[hep-ph/0702031](#)].
- [129] M. Wakamatsu and Y. Nakakoji, *Phenomenological analysis of the nucleon spin contents and their scale dependence*, *Phys. Rev. D* **77** (2008) 074011 [[0712.2079](#)].
- [130] J.-Y. Kim, H.-C. Kim, M.V. Polyakov and H.-D. Son, *Strong force fields and stabilities of the nucleon and singly heavy baryon Σ_c* , *Phys. Rev. D* **103** (2021) 014015 [[2008.06652](#)].
- [131] D. Diakonov, M.V. Polyakov and C. Weiss, *Hadronic matrix elements of gluon operators in the instanton vacuum*, *Nucl. Phys. B* **461** (1996) 539 [[hep-ph/9510232](#)].
- [132] J. Ossmann, M.V. Polyakov, P. Schweitzer, D. Urbano and K. Goeke, *The Generalized parton distribution function $(E^{*u} + E^{*d})(x, xi, t)$ of the nucleon in the chiral quark soliton model*, *Phys. Rev. D* **71** (2005) 034011 [[hep-ph/0411172](#)].
- [133] J.-Y. Kim, *Quark distribution functions and spin-flavor structures in $N \rightarrow \Delta$ transitions*, [2305.12714](#).
- [134] D. Diakonov, V.Y. Petrov and P.V. Pobylitsa, *A Chiral Theory of Nucleons*, *Nucl. Phys. B* **306** (1988) 809.
- [135] M. Wakamatsu and Y. Nakakoji, *Generalized form factors, generalized parton distributions and the spin contents of the nucleon*, *Phys. Rev. D* **74** (2006) 054006 [[hep-ph/0605279](#)].
- [136] M. Wakamatsu and H. Tsujimoto, *The Generalized parton distribution functions and the nucleon spin sum rules in the chiral quark soliton model*, *Phys. Rev. D* **71** (2005) 074001 [[hep-ph/0502030](#)].
- [137] P. Schweitzer, *The Chirally odd twist three distribution function $e^{*\alpha}(x)$ in the chiral quark soliton model*, *Phys. Rev. D* **67** (2003) 114010 [[hep-ph/0303011](#)].
- [138] Y. Ohnishi and M. Wakamatsu, *πN sigma term and chiral odd twist three distribution function $e(x)$ of the nucleon in the chiral quark soliton model*, *Phys. Rev. D* **69** (2004) 114002 [[hep-ph/0312044](#)].
- [139] C. Weiss and J.-Y. Kim. to appear, 2023.
- [140] J.-Y. Kim, U. Yakhshiev and H.-C. Kim, *Medium modification of the nucleon mechanical properties: Abel tomography case*, *Eur. Phys. J. C* **82** (2022) 719 [[2204.10093](#)].
- [141] H.-Y. Won, H.-C. Kim and J.-Y. Kim, *Role of strange quarks in the D-term and cosmological constant term of the proton*, [2307.00740](#).
- [142] J.Y. Panteleeva and M.V. Polyakov, *Forces inside the nucleon on the light front from 3D Breit frame force distributions: Abel tomography case*, *Phys. Rev. D* **104** (2021) 014008 [[2102.10902](#)].
- [143] J.-Y. Kim and H.-C. Kim, *Energy-momentum tensor of the nucleon on the light front: Abel tomography case*, *Phys. Rev. D* **104** (2021) 074019 [[2105.10279](#)].
- [144] A. Freese and G.A. Miller, *Forces within hadrons on the light front*, *Phys. Rev. D* **103** (2021) 094023 [[2102.01683](#)].
- [145] J.-Y. Kim, *Electromagnetic multipole structure of a spin-one particle: Abel tomography case*, *Phys. Rev. D* **106** (2022) 014022 [[2204.08248](#)].
- [146] J.-Y. Kim, B.-D. Sun, D. Fu and H.-C. Kim, *Mechanical structure of a spin-1 particle*, *Phys. Rev. D* **107** (2023) 054007 [[2208.01240](#)].

- [147] J.-M. Suh, J.-Y. Kim, G.-S. Yang and H.-C. Kim, *Quark spin content of $SU(3)$ light and singly heavy baryons*, *Phys. Rev. D* **106** (2022) 054032 [[2208.04447](#)].